

Review

Open Access



Enantioselective photochemical reactions within the confined cavities of supramolecular assemblies

Yi-Wen Su^{1,#}, Cheng Pan^{1,#}, Tao-Yue Sun¹, You-Quan Zou^{1,2,3,*} 

¹Department of Radiation and Medical Oncology, Zhongnan Hospital of Wuhan University, School of Pharmaceutical Sciences, Wuhan University, Wuhan 430071, Hubei, China.

²Key Laboratory of Combinatorial Biosynthesis and Drug Discovery, Ministry of Education, Wuhan University, Wuhan 430071, Hubei, China.

³TaiKang Center for Life and Medical Sciences, Wuhan University, Wuhan 430071, Hubei, China.

#Authors contributed equally.

*Correspondence to: Prof. You-Quan Zou, Department of Radiation and Medical Oncology, Zhongnan Hospital of Wuhan University, School of Pharmaceutical Sciences, Wuhan University, 185 Donghu Road, Wuhan 430071, Hubei, China. E-mail: youquanzou@whu.edu.cn

How to cite this article: Su, Y. W.; Pan, C.; Sun, T. Y.; Zou, Y. Q. Enantioselective photochemical reactions within the confined cavities of supramolecular assemblies. *Chem. Synth.* 2025, 5, 10. <https://dx.doi.org/10.20517/cs.2024.64>

Received: 22 May 2024 **First Decision:** 2 Jul 2024 **Revised:** 31 Jul 2024 **Accepted:** 7 Aug 2024 **Published:** 16 Oct 2024

Academic Editor: Wei Li **Copy Editor:** Pei-Yun Wang **Production Editor:** Pei-Yun Wang

Abstract

Compared to bulk solvents, reactions in the confined spaces of supramolecular self-assemblies feature rate acceleration, high efficiency and substrate selectivity. These advantages lead to efficient catalytic efficiency and excellent selectivity in enantioselective supramolecular photochemical transformations. During the last few years, enantioselective supramolecular photocatalysis has developed into one of the most powerful strategies to construct enantioenriched chiral compounds. In this review, the recent advances of enantioselective photochemical reactions taking place within the confined spaces of supramolecular assemblies are summarized, with an emphasis on the specific catalytic modes and chemical transformations. Organization of the data follows a subdivision according to supramolecular host and reaction type. At last, the current limitations and the future research orientation of this research field are discussed.

Keywords: Supramolecular catalysis, enantioselective photochemistry, photocatalysis, confinement, host-guest interactions



© The Author(s) 2024. **Open Access** This article is licensed under a Creative Commons Attribution 4.0 International License (<https://creativecommons.org/licenses/by/4.0/>), which permits unrestricted use, sharing, adaptation, distribution and reproduction in any medium or format, for any purpose, even commercially, as long as you give appropriate credit to the original author(s) and the source, provide a link to the Creative Commons license, and indicate if changes were made.



INTRODUCTION

Enantioselective photochemical reaction represents a powerful and intriguing protocol to construct enantioenriched chiral compounds^[1-3]. In this regard, photochemical reactions take place in a chiral environment. Generally, there are two ways to realize enantioselective photochemical reactions. One is using a chiral photosensitizer (template) which can simultaneously initiate the photochemical reaction and induce the chirality of the terminal product. The other is a synergistic strategy where a photochemical process is mediated by an achiral photosensitizer and chiral transfer is controlled by another chiral catalyst (template). Nevertheless, some inherent challenges remain in the stereo-control of enantioselective photochemical reactions. For instance, the short lifetime and weak intermolecular interactions in electronically excited states complicate chiral transfer between a chiral template (catalyst) and substrate. Meanwhile, organic molecules in excited states have relatively high reactivity, leading to undesired transformations without interacting with the chiral template (catalyst).

Recently, supramolecular catalysis has generated increasing interest, whereby catalytic reactions can occur inside confined cavities - supramolecular containers and assemblies (hosts)^[4-13]. In 2010, Meeuwissen *et al.* highlighted that the implementation of supramolecular assemblies into transition-metal catalysis and organocatalysis exhibits promising catalytic potential beyond enzyme mimics^[14]. In contrast to bulk solvents, reactions in nanovessels feature (1) rate acceleration; (2) high efficiency; (3) substrate selectivity, which can be controlled at the microscopic level, as a consequence of the recognition and energetic stabilization of substrates (guests) and transition states within well-confined cavities^[15-20].

Supramolecular hosts assemble from multiple components via weak intermolecular interactions (e.g., van der Waals, hydrogen bonding, metal ion coordination, π -stacking and hydrophobic interactions), which can serve as well-organized tunable catalytic systems^[21]. Structurally, the host exhibits a certain degree of skeletal rigidity, and the inner lipid-soluble cavities can accommodate organic guests. This advantage creates a unique environment for the subsequent photochemically chiral transfer, avoiding the unfavorable impacts of external factors, i.e., solvent polarity, temperature and acidity/basicity, on the asymmetric induction. Supramolecular host-guest interactions can alter photophysical properties of guest molecules through the combined non-covalent forces and steric constraints. The non-covalent host and guest interactions in the ground state will complement the transient and weak excited-state interactions^[22]. The confinement of chiral supramolecular hosts plays a key role in pre-organizing the substrate by the manipulation of the orientation and conformation/configuration of the guest and inducing the process of enantio-differentiation and photochirogenesis^[23]. In light of these advantages, the rational design of novel supramolecular catalysts or platforms and studies of their applications in the asymmetric photocatalysis are a topic of great interest across academia and industry.

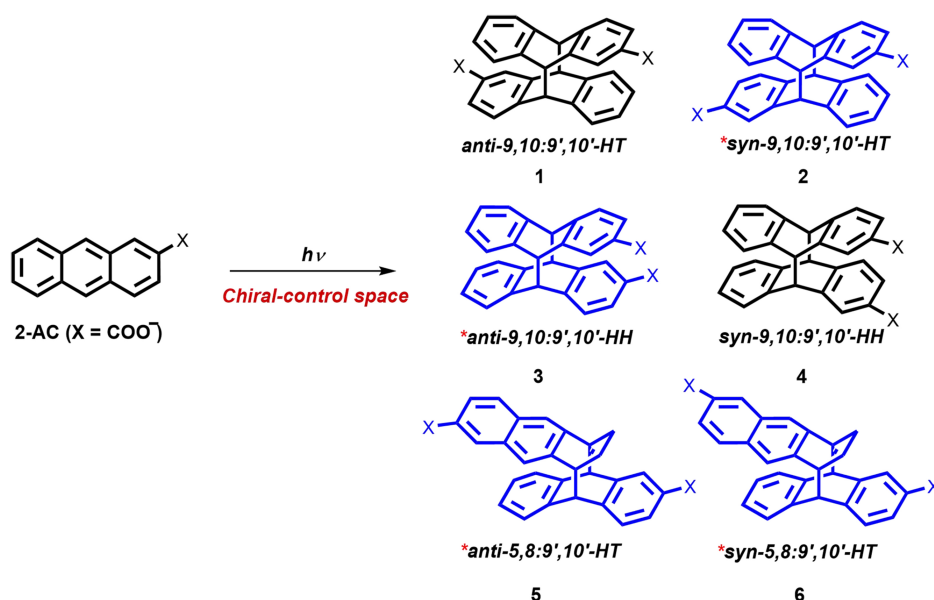
Over the past two decades, a plethora of supramolecular hosts have been developed to initiate the enantioselective photochemical reactions, including native and functionalized macrocycles, metal-organic cages (MOCs), metal-organic frameworks (MOFs), and covalent organic frameworks (COFs). Asymmetric photocatalytic transformations, such as photodimerization, photocyclization, photoisomerization, photocycloaddition, functionalization, and photooxidation reactions, have been well established using these supramolecular hosts. Table 1 summarized the hosts and enantioselective photoreactions discussed in this review. Reactions mediated by biomacromolecules (e.g., serum albumin and nucleic acids)^[24,25] and liquid crystals^[26,27] will not be discussed here. In this context, the review will provide a comprehensive summary of the recent advances in enantioselective photochemical reactions within the confined cavities of supramolecular assemblies, with an emphasis on the specific catalytic modes and types of chemical transformations. Due to different structural and physiochemical properties, these supramolecular hosts have

Table 1. Summary of the hosts and enantioselective photoreactions discussed in this review

Host type	Cavity	Reaction type	Guest category	Key role of cavity	Stereochemical outcome [ref.]
Macro-cycles	Native CDs	Photodimerization Photocyclization	ACs; naphthalenes Cyclic ketenes	Pre-organization Rigid environment	See Table 2 14 : 33% ee ^[45] ; 16 : 59% ee ^[46] ; 20 : 45% ee ^[48]
	Modified CDs	Photodimerization Photocyclization	ACs Adamantyl acetophenone	Pre-organization Chiral auxiliary	See Table 2 <i>cis</i> - 18 : 20% ee; <i>trans</i> - 18 : 9% ee ^[47]
	OA	Photodimerization	ACs	Pre-organization	2 : up to 67% ee; 3 : up to 56% ee ^[41]
	Photosensitizing hosts	Photoisomerization Photoaddition	Cyclooctene; cyclooctadiene Diphenylpropene	Activate substrate Activate substrate	Refer to ^[44] 22 : 26% ee ^[50]
MOCs	[Pd ₆ (RuL ₃) ₈] ²⁸⁺ (MOC-1)	Photodimerization	2-Naphthol	Stabilize product	25 : up to 58% ee ^[56]
			Unsymmetrical acenaphthylene	Energy transfer	27 : up to 88% ee ^[57]
		Photocycloaddition	Active olefins	Heteromolecular binding	33 : up to 99% ee ^[61]
MOFs	[Pd ₆ L ₄] ¹²⁺ (MOC-2)	Photocycloaddition	Fluoranthene and maleimide	Pre-organization	30 : 50% ee ^[59]
	MOF-3 (M = K)	Photodimerization	ACs	Multivalent interactions	47 : up to 79% ee ^[65]
	MOF-4 (M = Zn)	α -alkylation of aldehydes	Saturated aldehyde	Electron transfer and stereo-induction	52 : up to 92% ee ^[66]
	MOF-5 (M = Zn)	β -arylation of aldehydes	Saturated aldehyde	Electron transfer and stereo-induction	58 : up to 52% ee ^[67]
	MOF-6s (M = Zn, Zr, Ti)	α -alkylation of aldehydes	Saturated aldehyde	Electron transfer and stereo-induction	52 : up to 87% ee ^[68]
COFs	MOF-7,8,9,10				See Table 3
	COF-11, COF-12 (with chiral additive)	α -alkylation of aldehydes	Saturated aldehyde	Electron transfer and stereo-induction (exogenous)	65 : up to 94% ee ^[79]
	COF-13, COF-14 (with chiral additive)	α -alkylation of aldehydes	Saturated aldehyde	Electron transfer and stereo-induction (exogenous)	73 : up to 94% ee ^[80]
	COF-15 (chiral COF)	α -benzylation of aldehydes	Saturated aldehyde	Photothermal conversion and stereo-induction	65 : up to 94% ee ^[82]
	COF-16s (chiral COF)	α -alkylation of aldehydes	Saturated aldehyde	Electron transfer and stereo-induction	65 : up to 93% ee ^[83]
	COF-17 (chiral COF)	Photooxidation	Methylphenylsulfide	Energy transfer and stereo-induction and phase transfer	83 : up to 99% ee ^[84]
	COF-18 (chiral COF)	Henry reaction	Benzylic alcohol and nitromethane	Photothermal conversion and stereo-induction	86 : up to 98% ee ^[85]
	COF-19 (chiral COF)	A ³ -coupling	Benzaldehyde and aromatic alkyne and secondary amine	Photothermal conversion and stereo-induction	90 : up to 98% ee ^[85]
	COF-20 (chiral COF)	Strecker reaction	Benzaldehyde and trimethylsilyl cyanide and secondary amine	Photothermal conversion and Lewis acid catalysis and stereo-induction	94 : 94% ee ^[86]
	COF-21 (with enzyme)	Oxidative Mannich reaction	2-Arylindole	Energy transfer and stereo-induction (exogenous)	96 : 86% ee ^[87]

CDs: Cyclodextrins; ACs: anthracenes; OA: octa acid; MOCs: metal-organic cages; MOFs: metal-organic frameworks; COFs: covalent organic frameworks; LA: Lewis acid.

diverse functions in enantioselective photocatalysis. In order to help the readers understand the unique advantages of supramolecular strategy in photochirogenesis, we will try to elucidate the specific supramolecular effects of the hosts exerted on the reactions. Organization of the data follows a subdivision according to supramolecular host and reaction types. The current challenges and potential research orientations of this research field will also be discussed.



Scheme 1. The products of [4 + 4] photodimerization of 2-anthracenecarboxylate.

ENANTIOSELECTIVE PHOTOREACTIONS WITHIN MACROCYCLES

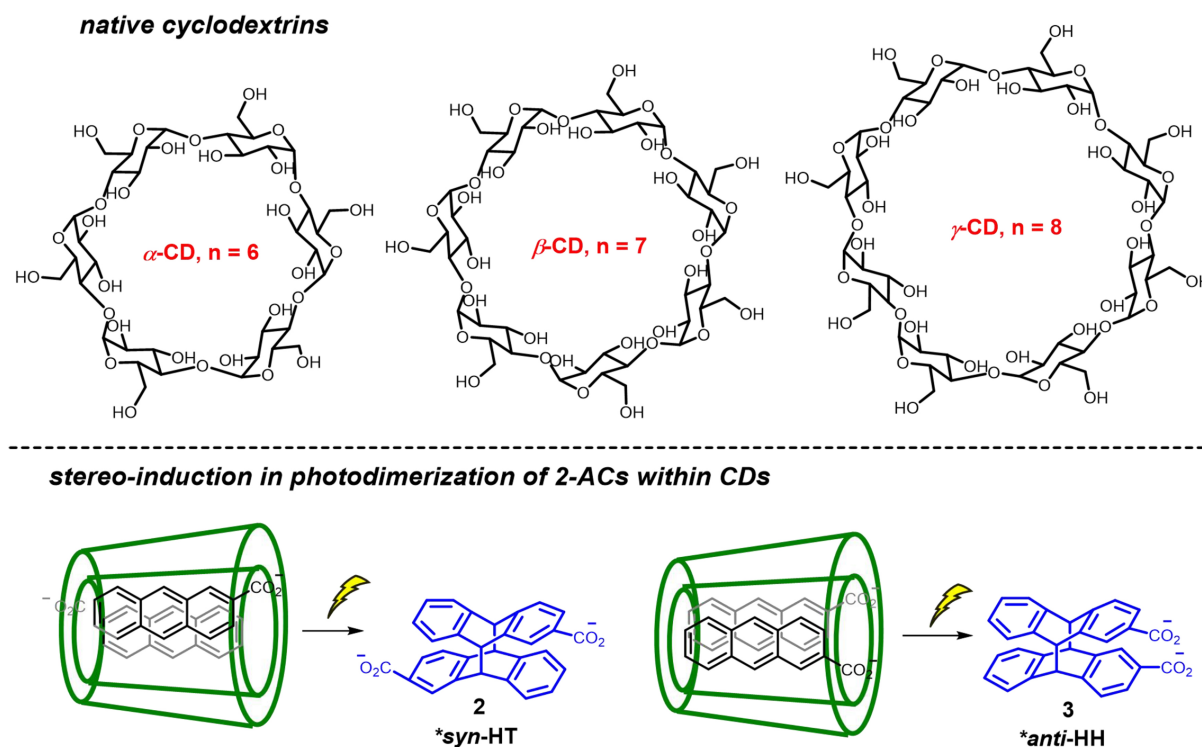
Macrocycles, especially composed of repeated glucose units, are the earliest supramolecular hosts to be used for asymmetric photoreactions. This kind of macrocycle features visible-light transparency, flexible modification and chiral cavities. In this section, enantioselective photodimerization, photoisomerization and several other types of photochemical transformations within macrocyclic hosts will be discussed.

Photodimerization within macrocyclic hosts

The selective [4 + 4] photodimerization of arenes within macrocycles is a long-standing research topic in supramolecular photochemistry. In this context, cyclodextrins (CDs) are always introduced as the chiral hosts. Anthracenes (ACs) are the most selected substrates to evaluate the photochirogenic ability and catalytic performance of a chiral supramolecular macrocycle^[28]. Generally, the irradiation of 2-anthracenecarboxylate will afford four configurational isomers [Scheme 1], among which *syn*-9,10:9'10'-head-to-tail dimer 2 (*syn*-HT) and *anti*-9,10:9'10'-head-to-head dimer 3 (*anti*-HH) are chiral, while *anti*-9,10:9'10'-head-to-tail (*anti*-HT) and *syn*-9,10:9'10'-head-to-head (*syn*-HH) cyclodimers 1 and 4 are achiral. Studies have also shown that the chiral slipped cyclodimers 5 and 6 (*anti*-5,8:9',10'-HT, *syn*-5,8:9',10'-HT) can also be generated^[29]. In this part, the related work in this field will be presented in chronological order.

Native CDs and modified CDs

As shown in Scheme 2, CDs are cyclic oligosaccharides containing D-glucose units linked via α -1,4 glycosidic bonds. Three kinds of native CDs, α -CD ($n = 6$), β -CD ($n = 7$), and γ -CD ($n = 8$), are formed with different numbers of glucose units. CDs bear two portals after assembling into a truncated funnel: a wider portal containing secondary hydroxyl groups and a narrow one comprising primary hydroxyl groups. Guest molecules will enter the hydrophobic cavity of the host upon complexation, while polar or charged functionalities reside outside. CDs feature chiral cavities, ready availability, good solubility in water as well as transparency in ultraviolet-visible (UV-vis) regions. The chiral confinement of CDs leads to a hydrophobic environment, substrate proximity, increased local concentration, and substrate pre-organization, which have been widely used to promote the reactivity and manipulate the selectivity^[30]. Accordingly, CDs and modified CDs have become the foremost hosts for asymmetric [4 + 4]



Scheme 2. The chemical structures of native CDs (top) and stereo-induction in the photodimerization of 2-ACs within CDs (bottom). CDs: Cyclodextrins; ACs: anthracenes.

photodimerization of AC derivatives [Scheme 3]. For a clear comparison, the stereochemical outcomes of photodimerization of AC within native and modified CDs have been summarized in Table 2.

To achieve excellent stereo-control, rigid and flexible caps or cationic side arms were always installed into γ -CD to pre-organize the guest molecules 2-ACs via multiple intermolecular interactions. In 2003, Nakamura and Inoue reported the generation of a 1:2 inclusion complex between γ -CD and AC could accelerate the photodimerization^[31]. The enantiomeric excess (*ee*) of the *syn*-HT dimer was 32% at 25 °C, which was increased to 41% by lowering the temperature to 0 °C (46% yield). In contrast, the *ee* of *anti*-HH dimer was less than 5%. Later, they found that installing a cationic side arm (CD-1) or a rigid cap (CD-2) into γ -CD could further improve the *ees* of *syn*-HT and *anti*-HH dimers to 58% and 41%, respectively^[32,33].

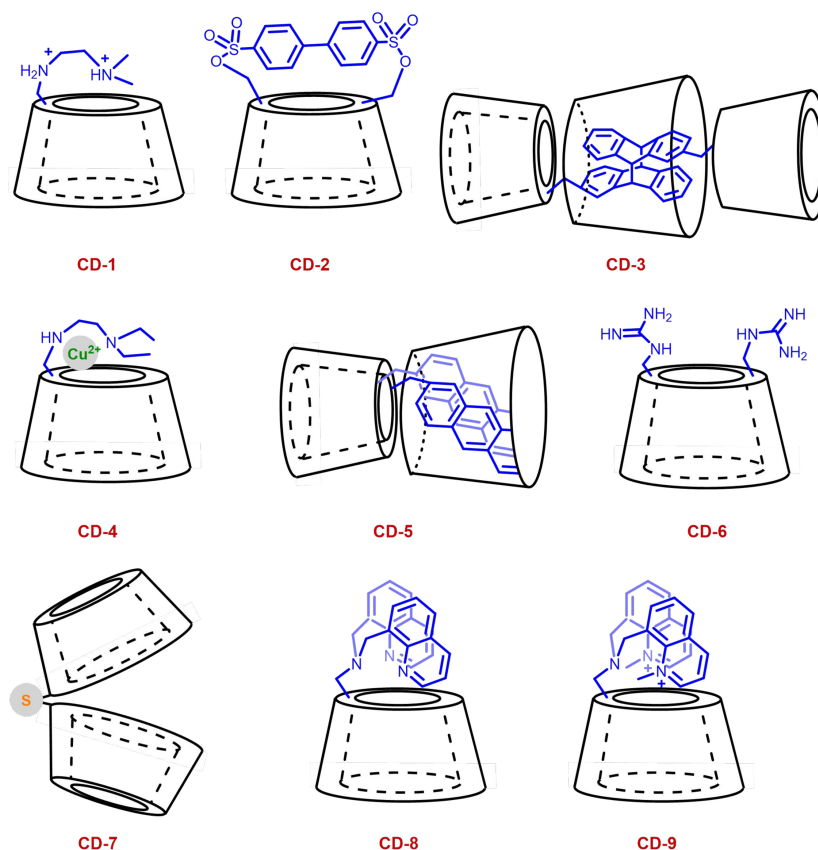
In 2008, Yang *et al.* synthesized α -CD-appended AC to investigate the stereodifferentiating photodimerization within γ -CD (CD-3) and cucurbit[8]uril (CB[8])^[34]. Interestingly, the head-to-tail (HT) dimers were formed in 98% selectivity within CD-3. Particularly, the *syn*-HT photodimer was generated in 68% yield with 91% *ee*, which were much higher than the reaction with unmodified AC carboxylate (32% *ee*, 44% yield). An inversion of HT/head-to-head (HH) selectivity was also observed using CB[8], affording exclusively the HH photodimers (99% selectivity). This study indicated that the outside interactions can influence the asymmetric photochemical reaction by manipulating the ground-state complexation and the excited-state reactivity.

Shortly after, a non-sensitizing metallocuprasupramolecular host (CD-4) consisting of diamino- γ -CD combined with $\text{Cu}(\text{ClO}_4)_2$ was exploited by Ke *et al.* to promote the photodimerization of AC^[35]. In this study, the *anti*-HH dimer formed in 51%-52% yields with 64%-70% *ees* within CD-4 at -50 °C in aqueous methanol.

Table 2. Stereochemical outcomes of photodimerization of 2-ACs within native and modified CDs in Scheme 3

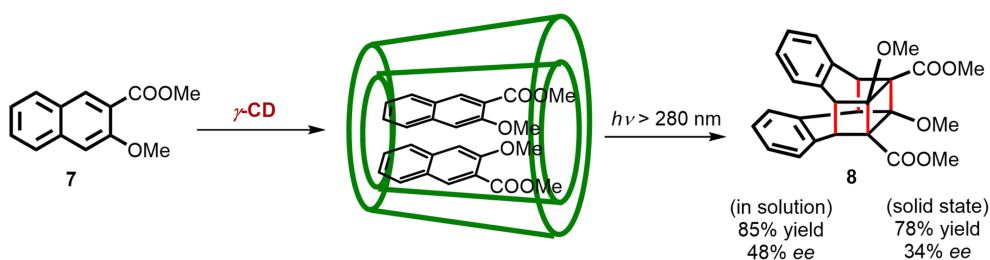
CD host	Regioselectivity HT/HH	Enantioselectivity		Temperature (°C)
		<i>syn</i> -HT 2 (ee %)	<i>anti</i> -HH 3 (ee %)	
γ -CD ^[31]	8.3/1	41%	< 5%	0
CD-1 ^[32]	1/2.9	3%	41%	-59
CD-2 ^[33]	2/1	58%	14%	0
CD-3 ^[34]	-1/0	91%	2%	-20
CD-4 ^[35]	1/4	13%	70%	-50
CD-5 ^[37]	-0/1	-	99%	-18
CD-6 ^[38]	1/6.7	52%	86%	-85
CD-7 ^[39]	-1/0	> 99%	-	-20
CD-8 ^[40]	1.2/1	41%	64%	-20
CD-9 ^[40]	0.9/1	30%	76%	-20

ACs: Anthracenes; CDs: cyclodextrins; HT: head-to-tail; HH: head-to-head.

**Scheme 3.** Representative modified CDs employed in enantioselective photodimerization of 2-ACs. CDs: Cyclodextrins; ACs: anthracenes.

Mechanistically, the CD-4 facilitates the generation of a HH-oriented 1:2 host-guest complex and discourages the generation of the diastereomeric *syn*-HH complex.

Luo *et al.* studied the photodimerization of naphthalene derivatives in native γ -CD [Scheme 4]^[36]. Unlike AC, naphthalene 7 underwent a photodimerization and produced the *anti*-HH cubane-like product, which usually could not be obtained under thermal reaction conditions. In this study, the *anti*-HH photodimerization product 8 was generated in 48% (aqueous solution) and 34% (solid state) *ee* under



Scheme 4. Enantioselective photodimerization of naphthalene derivatives.

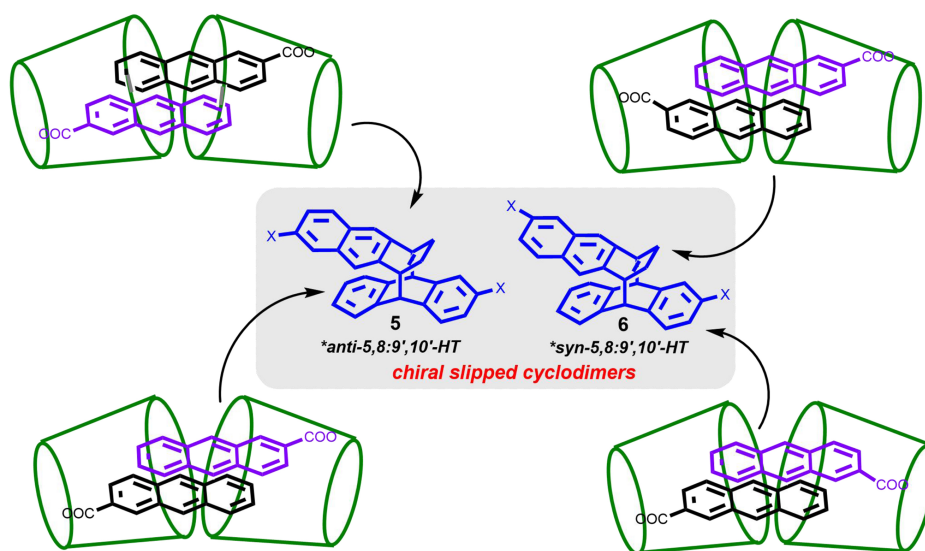
ambient temperature and pressure.

In 2011, Yang *et al.* developed an enantioselective photochemical protocol to realize the acceleration and excellent stereo-control in the photodimerization of 2-anthracenecarboxylate tethered to an α -CD scaffold^[37]. In this protocol, two AC molecules tethered to one α -CD (**CD-5**) were accommodated in the cavity of γ -CD or CB[8]. The *anti*-HH dimer was selectively obtained in 98% yield with 99% *ee* using γ -CD as the host, while 97% yield and 98% *ee* were recorded in achiral CB[8].

To better manipulate the stereochemical outcomes of [4 + 4] photodimerization of ACs, Yao *et al.* synthesized several diamino- γ -CD and diguanidino- γ -CD hosts^[38]. In the photodimerization mediated by diguanidino- γ -CD (CD-6), they found the *ee* and chiral sense of the final products were dynamic functions of reaction temperature and the co-solvent. The *anti*-HH dimerization product was generated with moderate enantioselectivity in aqueous methanol at -70 °C (64% *ee*), while the antipodal isomer was formed in 72% yield with excellent enantioselectivity at -85 °C in aqueous ammonia (86% *ee*). However, the diamino- γ -CD host did not exhibit this remarkable stereo-control behavior.

The above studies mainly focused on the modifications of larger-in-cavity γ -CD to mediate photodimerization of ACs and deliver classical chiral 9,10:9'10'-cyclodimer products. The slipped chiral cyclodimers have long been overlooked. In 2018, Wei *et al.* disclosed that chiral slipped 5,8:9',10'-cyclodimers **5** and **6** were produced by β -CD via higher-order 2:2 complexation [Scheme 5]^[29]. The authors also investigated the photophysical and structural aspects of the complexation-mediated transformation. Later, Ji *et al.* designed and prepared a range of sulfur-linked or arene-spacer-tethered β -CD dimers (CD-7) for manipulating the enantio- and regioselectivities of the photochemical dimerization of 2-AC^[39]. In this system, two nonclassical 5,8:9',10'-cyclodimers (**5** and **6**) and four stereoisomeric classical 9,10:9'10'-cyclodimers were generated via a photoreactive 1:2 complex. Wherein *syn*-9,10:9'10'-HT dimer could be obtained in 98% yield with > 99% *ee*.

The enantiomeric forms of CD compounds are not readily available. Therefore, preparation of the enantiomers of chiral products through the induction of opposite chirality is not relevant in CD-mediated transformation. Variation of external factors, such as temperature, solvent, irradiation wavelength, pH and additives, and modification of CD frameworks may lead to chirality inversion of CD-mediated asymmetric photochemical reactions. For instance, Kanagaraj *et al.* harnessed two types of γ -CD derivatives, videlicet, bisquinoline-modified γ -CD (**CD-8**) and its *N*-methylated derivative (**CD-9**) to catalyze the photodimerization of 2-anthracenecarboxylic acid^[40]. By adjusting the pH, the *ee* of the *anti*-HH dimer was inverted from 25% to -64% (within **CD-8**) and 41% to -76% (within **CD-9**), respectively.



Scheme 5. The formation of slipped cyclodimers via 2:2 host-guest complexation.

Other macrocyclic hosts

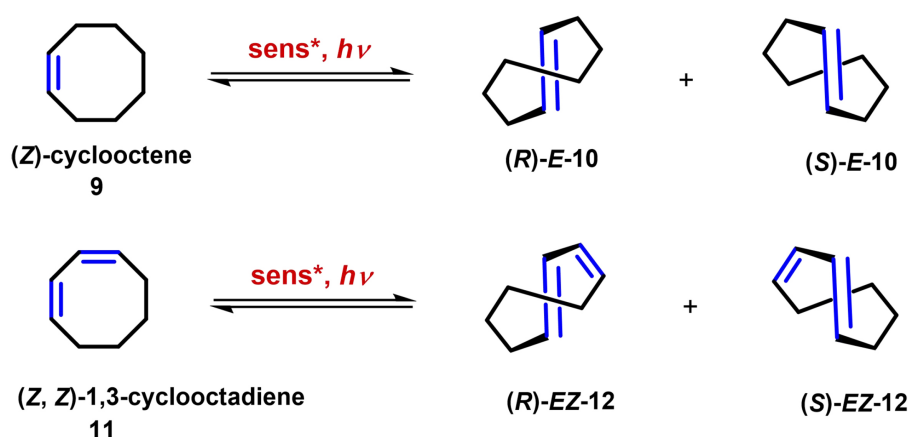
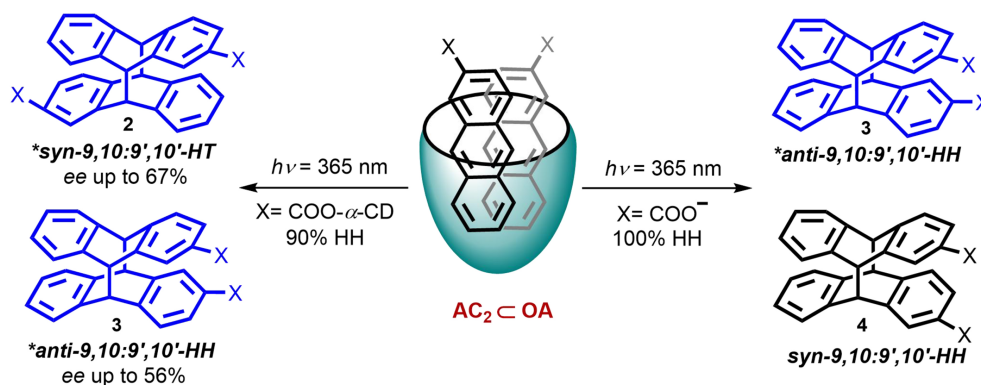
Apart from above CD-based hosts, organic macrocyclic octa acid (OA) is also suitable for enantioselective photodimerization of 2-AC. In 2020, Wei *et al.* found that OA can act as both a capsule and a cavitand^[41]. As shown in [Scheme 6](#), the AC molecules were oriented with the two COO⁻ groups facing water and the two AC rings buried within the hydrophobic cavity of the cavitand. Interestingly, photodimerization with this cavitand favored a HH dimer product. In addition, when guests were tethered with a chiral auxiliary (α -CD-AC), achiral OA can also induce this photodimerization reaction with good diastereoselectivity.

Photoisomerization within macrocyclic hosts

Photoisomerization of (*Z*)-cyclooctene **9** and (*Z,Z*)-1,3-cyclooctadiene **11** can also take place inside the cavity of macrocyclic supramolecular hosts, furnishing the desired chiral products (*R/S*)-(*E*)-cyclooctene **10** and (*R/S*)-(*E,Z*)-1,3-cyclooctadiene **12**, respectively [[Scheme 7](#)]^[42,43]. In this context, modified oligosaccharide supramolecular hosts, such as aryl-derived CD hosts and functionalized cyclic nigerosynigerose (CNN), have been introduced to mediate this transformation. Due to the fact that neither cyclooctene nor cyclooctadiene can absorb the light, functionalization of these macrocyclic hosts with various photosensitizers is essential. These modified macrocycles can serve as a chiral photosensitizer to activate the substrate and manipulate the enantioselectivity simultaneously. Compared with the transformation in bulk solvents, enantioselective photoisomerization of cyclooctene/cyclooctene within supramolecular cavities can proceed in the aqueous environment and achieve promising enantioselectivity under relatively mild reaction conditions. Related works in this research field have been nicely summarized by Genzink *et al.*^[44]. Therefore, we will not highlight this aspect herein.

Other transformations within macrocyclic hosts

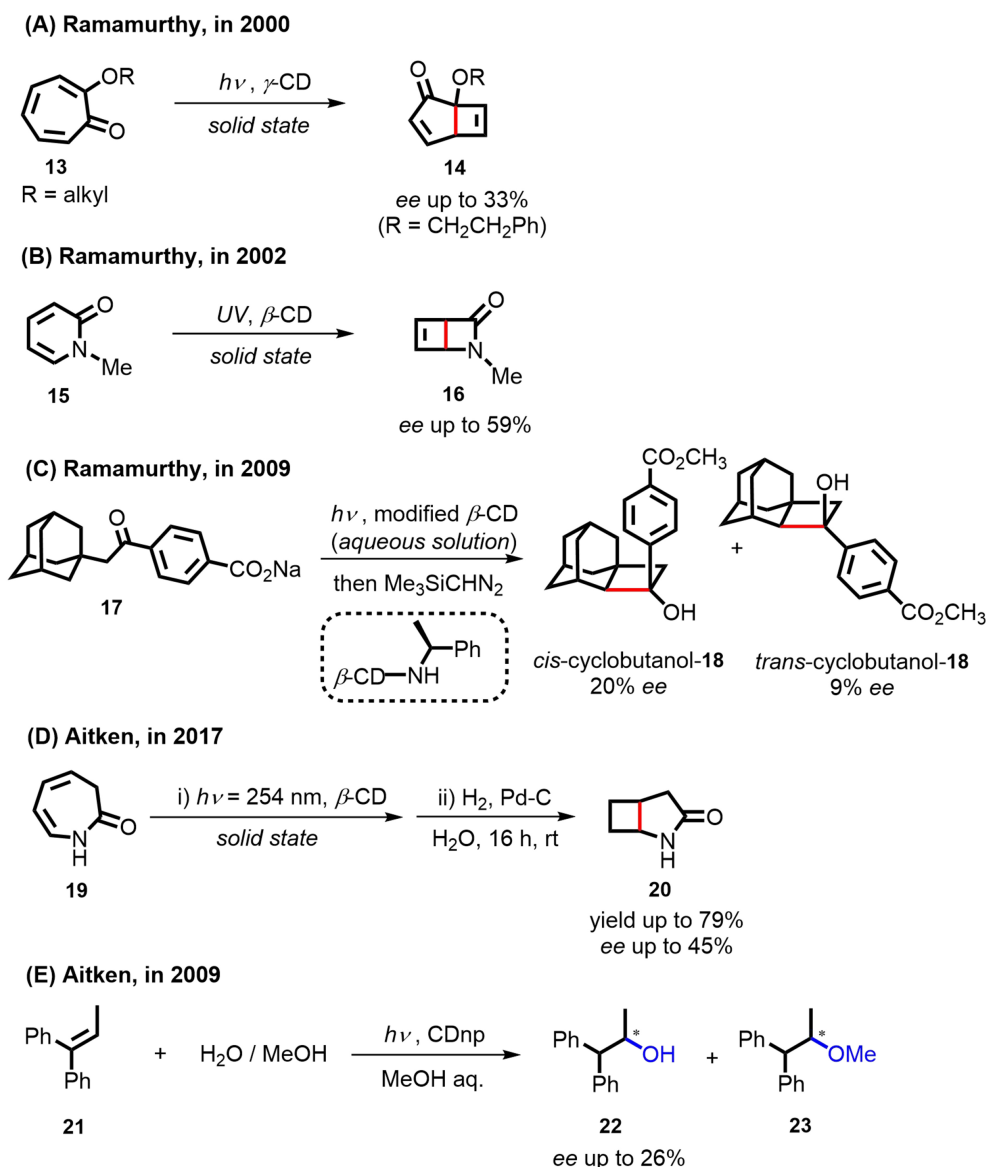
Several other types of enantioselective photochemical reactions mediated by macrocycles have also been studied, including [2 + 2] photocycloaddition reaction, photocyclization and difunctionalization of alkenes. For instance, Koodanjeri *et al.* employed CDs in the photocyclization of achiral tropolone alkyl ethers **13** to yield a bicyclo[3.2.0] product **14** bearing two contiguous chiral centers (up to 33% *ee*) [[Scheme 8A](#)]^[45]. Subsequently, the same group reported a β -CD-mediated photocyclization of achiral *N*-alkyl pyridones **15** to 2-azabicyclo[2.2.0]-hex-5-en-3-ones **16** with up to 59% *ee* in the solid state [[Scheme 8B](#)]^[46]. In 2009, they further studied the chiral induction by β -CD in intramolecular photocyclization of carbonyl compounds^[47].



Taking the photocyclization of adamantyl acetophenone **17** as an example, *trans*-cyclobutanol and *cis*-cyclobutanol **18** were obtained in 9% and 20% *ee*, respectively, in the presence of chiral benzylamine-derived β -CD [Scheme 8C]. Moreover, Mansour *et al.* utilized β -CD to mediate the photochemical electrocyclicization of 1,3-dihydro-2H-azepin-2-one **19** [Scheme 8D]^[48]. The authors found that no enantioselectivity was recorded in solution. However, solid-state [2 + 2] photocycloaddition followed by reduction delivered the terminal (1*R*,5*R*)-2-azabicyclo[3.2.0]heptan-3-one **20** in up to 79% isolated yields and with up to 45% *ee*.

On the other hand, Fukuhara *et al.* reported an enantioselective photochemical addition of methanol to 1,1-diphenylpropene (DPP) initiated by a cyanonaphthalene-modified β -CD (CDnp), affording *anti*-Markovnikov adducts^[49]. They further investigated the competitive addition of water and methanol to DPP in the presence of CDnp. In this study, the *ee* of water addition product **22** was up to 26% [Scheme 8E]^[50].

The above examples show that CD-based macrocycles are promising chiral hosts for enantioselective photodimerization of 2-anthracenecarboxylates and photoisomerization of cycloolefins. Asymmetric [2 + 2] photocycloaddition reaction, photocyclization and difunctionalization of alkenes using CDs also work, albeit with lower enantioselectivity. The chiral confinement of CD hosts plays a significant role in the pre-organization of the substrates in the ground state, which leads to not only the closer substrate proximity but also selective spatial arrangement of the guest molecules.



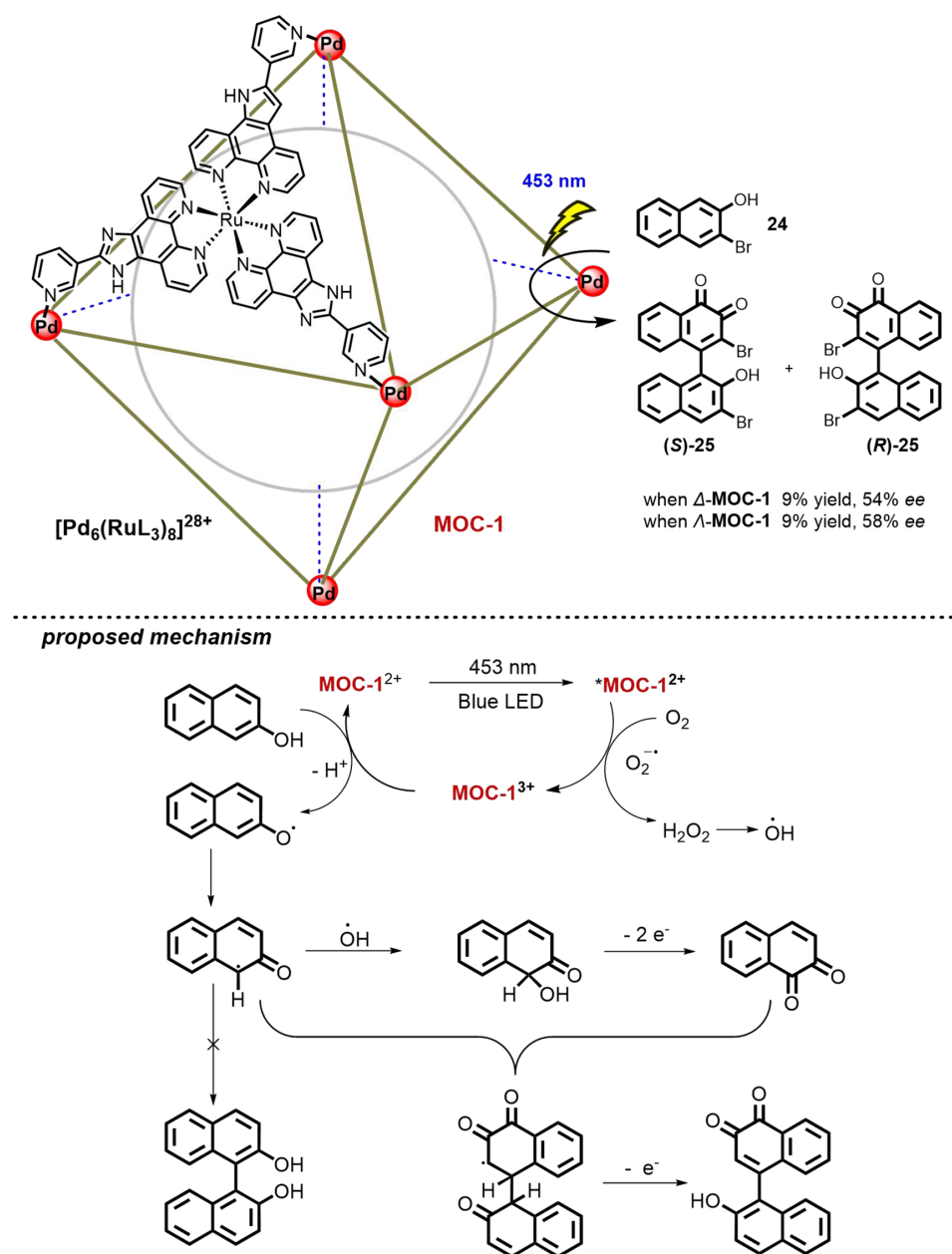
Scheme 8. Other asymmetric transformations within macrocyclic CD-based hosts. CD: Cyclodextrin.

ENANTIOSELECTIVE PHOTOREACTIONS WITHIN MOCS

Different from macrocycles, MOCs are assembled from metals and organic ligands through coordination^[51–53]. Recently, some chiral MOCs have been successfully introduced into enantioselective photocatalysis. In these studies, MOCs serve as efficient nanoreactors to utilize the light energy and induce the asymmetric photochemical reactions. This section will discuss the recent progress in enantioselective photodimerization and photocycloaddition reactions using chiral MOCs.

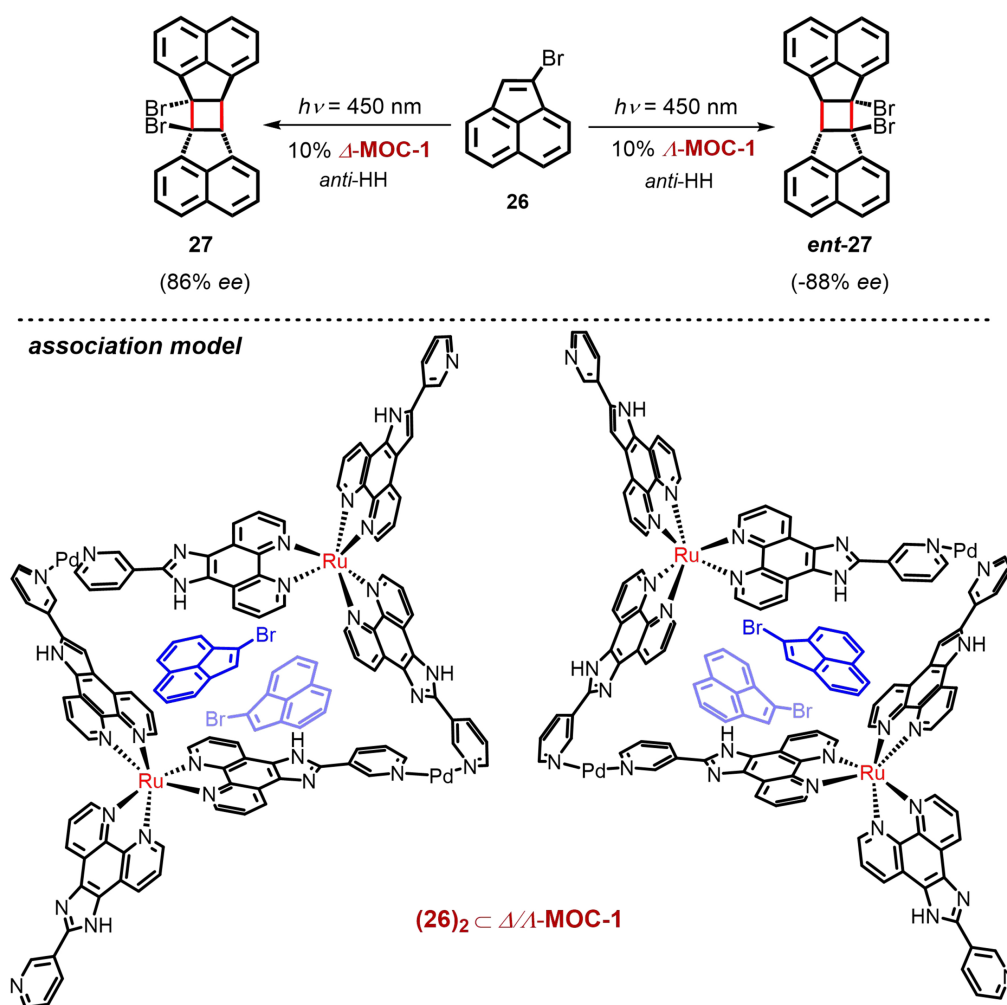
Photodimerization within MOCs

In 2014, Li *et al.* constructed a heterometallic [Pd₆(RuL₃)₈]²⁸⁺ MOC host (MOC-1), which incorporated photoredox-active and stereogenic RuL₃ units and supramolecular RuL₃/Pd photo-hydrogen-evolving (PHE) moieties^[54]. Further endeavors allowed them to obtain the homochiral and photoactive MOC-1 (*Δ/Δ*-MOC-1) with a chiral coordination space^[55]. Subsequently, Guo *et al.* reported a seminal work about regio-



Scheme 9. Regio- and enantioselective 1,4-homocoupling of 2-naphthol derivatives within Δ/Λ -MOC-1. MOC: Metal-organic cage.

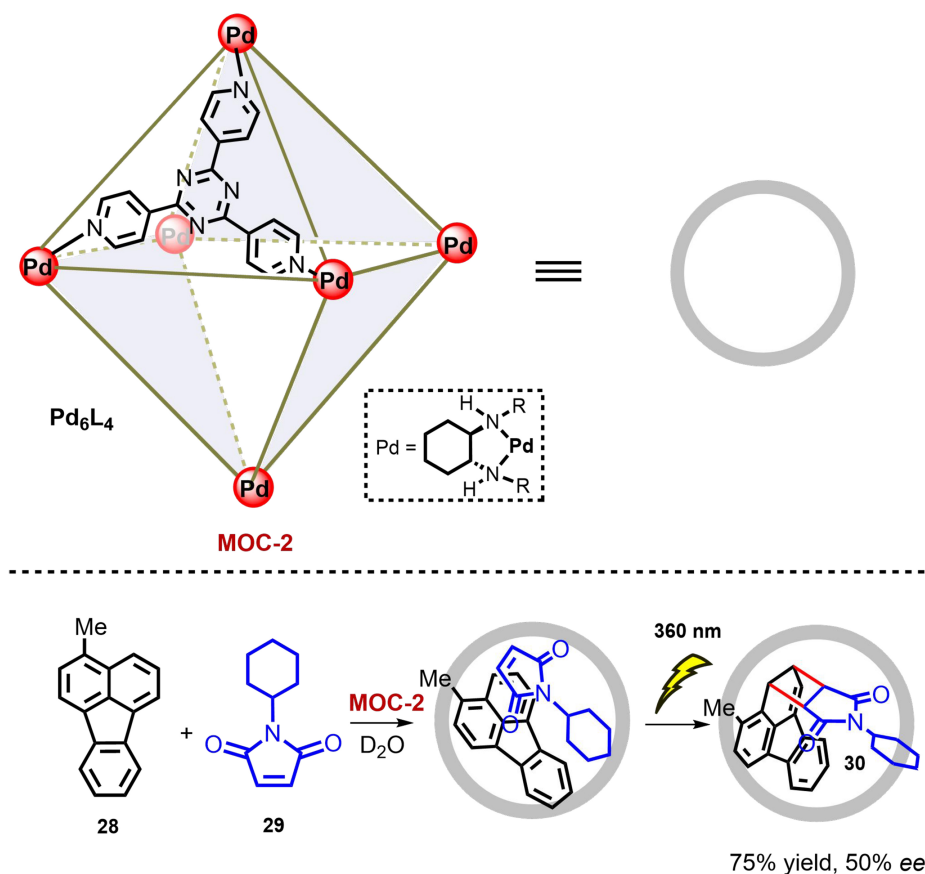
and enantioselective 1,4-homocoupling of 2-naphthol derivatives to form 4-(2-hydroxy-1-naphthyl)-1,2-naphthoquinone in the confined chiral-control cavity of Δ/Λ -MOC-1 [Scheme 9]^[56]. In most cases, the dimerization of 2-naphthols will generate relatively stable 1,1'-homocoupling product 1,1'-bi-2-naphthol (BINOL), with unstable 1,4-homocoupling product 25 as a side product. Under the optimized reaction conditions, 1,4-homocoupling product 25 was obtained in 54% (Δ -MOC-1) and 58% (Λ -MOC-1) ee with 5 mol% of Δ/Λ -MOC-1. Based on some spectral studies and theoretical calculations, a plausible mechanism was proposed. Upon the irradiation of blue light-emitting diodes (LEDs, 453 nm), MOC-1 was excited to the excited state ^{*}MOC-1²⁺, which was then quenched by O₂ to give MOC-1³⁺. Meanwhile, H₂O₂ formed via the reduction of the O₂ could easily produce hydroxyl radicals. Then, MOC-1³⁺ would oxidize the 2-naphthol via single electron transfer (SET) to give a 2-naphthol radical, which combined with a hydroxyl radical to generate the



Scheme 10. Enantioselective [2 + 2] photodimerization of acenaphthylene derivatives within Δ/Δ -MOC-1. MOC: Metal-organic cage.

naphthalene-1,2-dione intermediate. Finally, the coupling of a 2-naphthol radical and naphthalene-1,2-dione yielded the desired product. Owing to the constrained cage effects and host-guest chiral recognition and matching, Δ/Δ -MOC-1 could manipulate the stereoselectivity and stabilize the unstable configuration of the 1,4-homocoupling product. On the other hand, chiral-control space can also improve the coupling conversions by pre-organizing the substrates close to the ruthenium sites.

The [2 + 2] photodimerization of olefins has been extensively studied, which represents a feasible and efficient approach in the construction of cyclobutanes. Kindled by the pioneering work, Guo *et al.* reported an unprecedented [2 + 2] enantioselective photodimerization of an unsymmetrical acenaphthylene derivative **26** mediated by enantiopure Δ/Δ -MOC-1^[57]. The dimerization of **26** gave *anti*-HH product **27** both within Δ -MOC-1 (86% ee) and Δ -MOC-1 (-88% ee) with high regio-, stereo-, and enantioselectivity. In this transformation, the chiral confinement of Δ/Δ -MOC-1 played a pivot role in governing the stereochemical outcome. The combination of multiple functions, including the pre-organization of substrates in the ground state, the regulation of excited-state stereochemistry as well as the transfer of triplet energy and chirality, have been verified by experimental results and computational studies. As shown in Scheme 10, they have established the possible simplified cage models to deduce the most stable configurations of reactants and products associated with the cage to explain the high enantioselectivity.

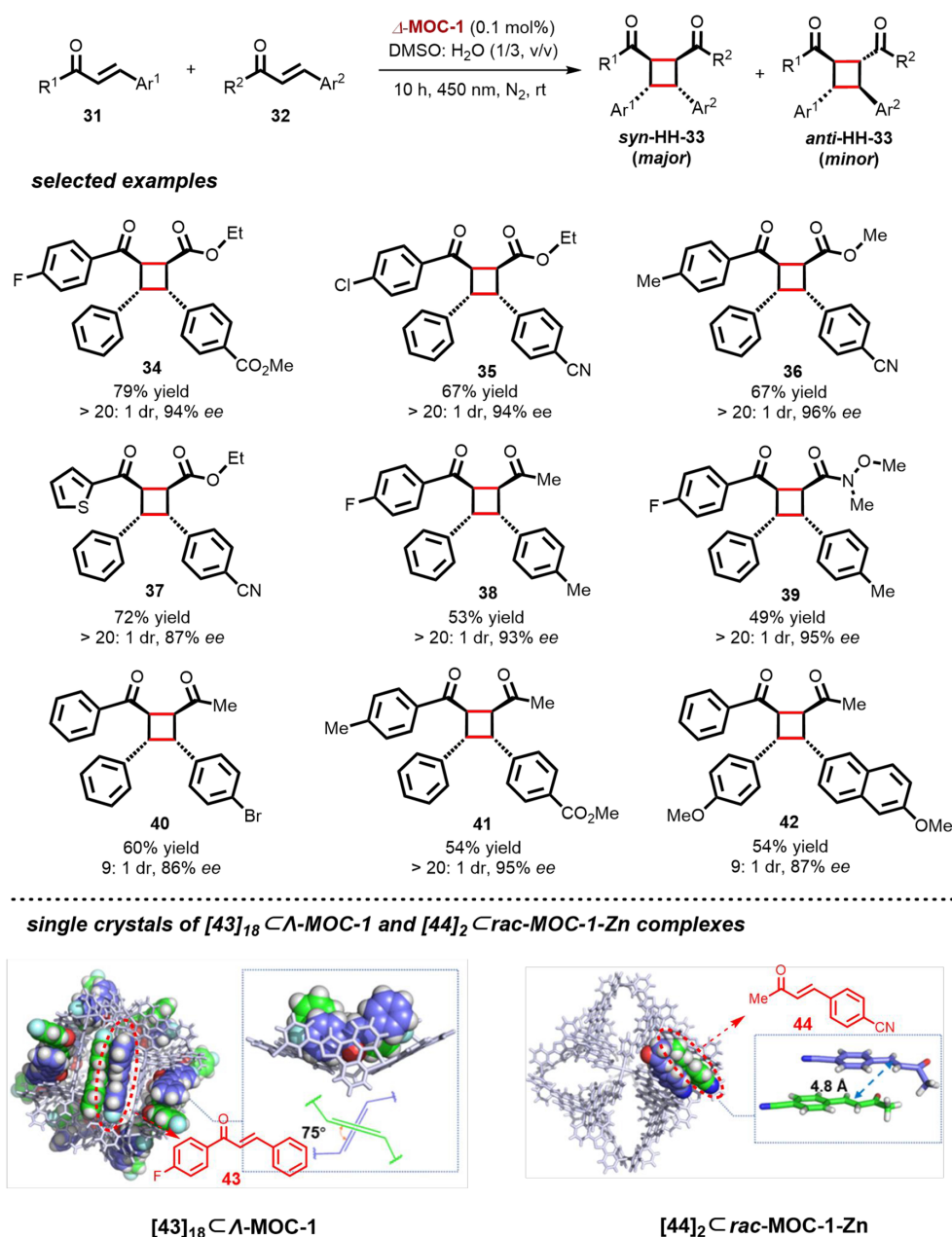


Scheme 11. Enantioselective [2 + 2] photocycloaddition of fluoranthene with maleimide within **MOC-2**. MOC: Metal-organic cage.

Photocycloaddition within MOCs

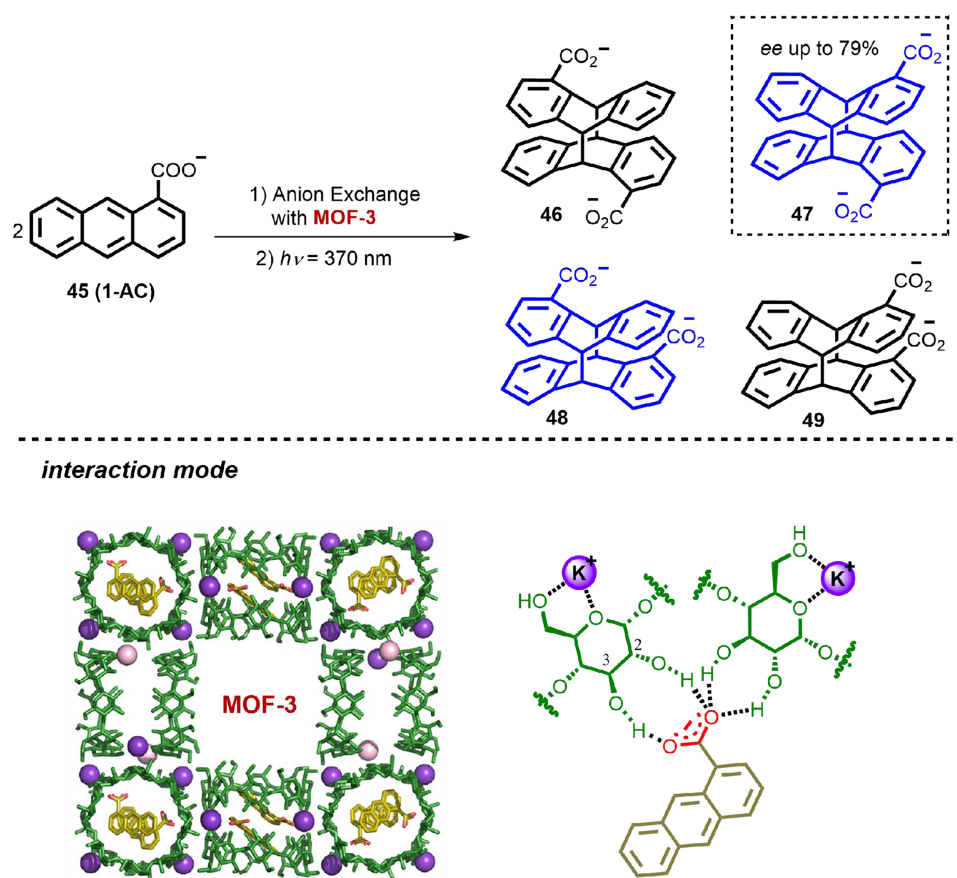
In 2006, Yoshizawa *et al.* prepared a self-assembled coordination cage (M_6L_4) by mixing an *exo*-tridentate ligand and an end-capped Pd^{II} ion in water^[58]. They found that the Diels-Alder reaction between AC and phthalimide occurred inside of this M_6L_4 cage with excellent regioselectivity. Subsequently, replacing the ethylenediamine with chiral diamines on each Pd center formed the chiral MOC (**MOC-2**) [Scheme 11]^[59]. They used **MOC-2** as a chiral host for the [2 + 2] photocycloaddition reaction of fluoranthene **28** with maleimide **29**. To their delight, the modification at the periphery of **MOC-2** was sufficient to produce considerable asymmetric induction. Upon the irradiation of 360 nm light, cyclobutane product **30** was obtained in 75% yield with 50% *ee*. **MOC-2** exhibited excellent guest binding capability, which worked as the prerequisite for the pre-organization of substrates at the ground state. Based on the calculation results, the authors ascribed the high regioselectivity to the steric effect within the confined cavity rather than orbital control. The control experiments suggested that the steric profile of the diamine ligand was correlated with the *ee* of the product. This study utilized a chiral diamine ligand to assemble a photoactive supramolecular coordination cage. The diamine ligand first coordinated with the Pd center and then induced the chiral deformation of the cavity. Further investigations revealed that the larger steric bulk of the N-substituent (R) increased the tilt angle of the triazine ligand, resulting in the enhancement of enantioselectivity.

Based on the previous studies on the applications of **MOC-1** in the enantioselective 1,4-homocoupling, [2 + 2] photodimerization and Diels-Alder reaction^[60], Ruan *et al.* explored its catalytic potential in other chemical transformations. Recently, they successfully utilized ***Δ*-MOC-1** to catalyze the asymmetric [2 + 2]



Scheme 12. Multilevel-selective [2 + 2] cross-photocycloaddition of α,β -unsaturated carbonyl compounds within Δ -MOC-1. Reproduced with permission from ^[61]. Copyright 2024, American Chemical Society. MOC: Metal-organic cage.

photocycloaddition of chalcone and cinnamate derivatives with high levels of chemo-, regio-, diastereo-, and enantioselectivities [Scheme 12]^[61]. In comparison with well-established photocycloaddition between active and inactive olefins, the formation of two different diradical intermediates renders the selective [2 + 2] cross-photocycloaddition of two photoactive olefins with similar reactivities a considerable challenge, since it may result in a complex outcome for photocycloaddition with the generations of multiple undesired isomers. This chiral cage photoreactor has enabled the enantioselective [2 + 2] cross-photocycloaddition via multilevel-selectivity control to promote the formation of *syn*-HH isomer that is sterically and thermodynamically unfavorable in traditional conditions. Under the optimal conditions, a *syn*-HH isomer



Scheme 13. Enantioselective [4 + 4] photochemical dimerization of 1-AC within γ -CD containing MOF-3. Reproduced with permission from^[65]. Copyright 2021, American Chemical Society. AC: Anthracene; CD: cyclodextrin; MOF: metal-organic framework.

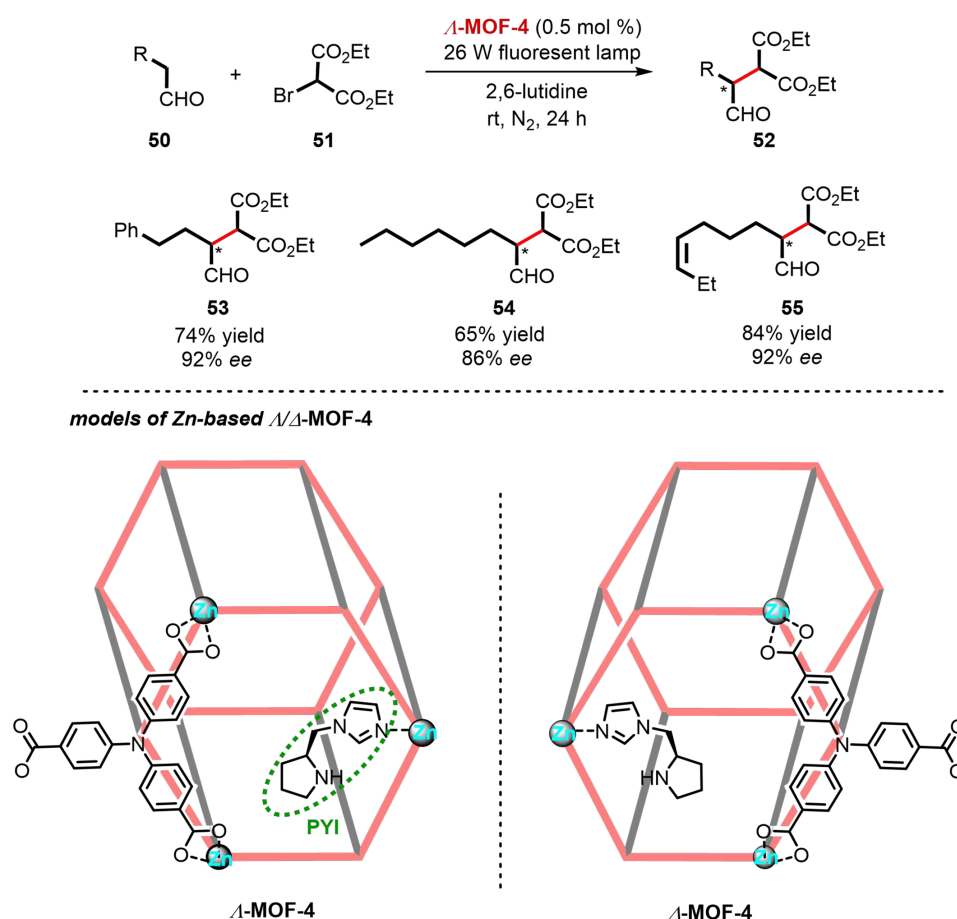
was obtained in good yield with excellent *ee* (39 examples, up to 86% yield and 99% *ee*). In this study, they obtained two single crystals of $[43]_{18} \subset A\text{-MOC-1}$ and $[44]_2 \subset rac\text{-MOC-1-Zn}$ complexes, both of which accommodate two same substrates in each pocket via π - π stacking interactions. It suggested that the distance (4.8 Å) or angle (75°) between the C=C bonds of the two same molecules is indeed unfavorable for homocoupling, which accounts for the preferential heterocoupling of two different substrates. Moreover, the controlled excited-state processes and dynamic exchange between the reactant and product within the cage reactor facilitated the formation of *syn*-HH cross coupling products. This study further demonstrated the advantages of supramolecular photochemical strategy in manipulating the chemoselectivity and stereoselectivity.

ENANTIOSELECTIVE PHOTOREACTIONS WITHIN MOFS

MOFs are a class of nanomaterials that feature high specific surface area and porosity, and easy functionalization^[62-64]. In recent years, some chiral MOFs have also been designed and employed in enantioselective photochemical reactions. In this part, asymmetric photodimerization, functionalization of aldehydes, and other intermolecular couplings within MOFs will be introduced.

Photodimerization within MOFs

In 2021, an elegant enantioselective [4 + 4] photodimerization of 1-AC[−] was reported by Chen *et al.* [Scheme 13]^[65]. Employing an anion-exchange protocol, 1-AC[−] was encapsulated inside the porous tunnels

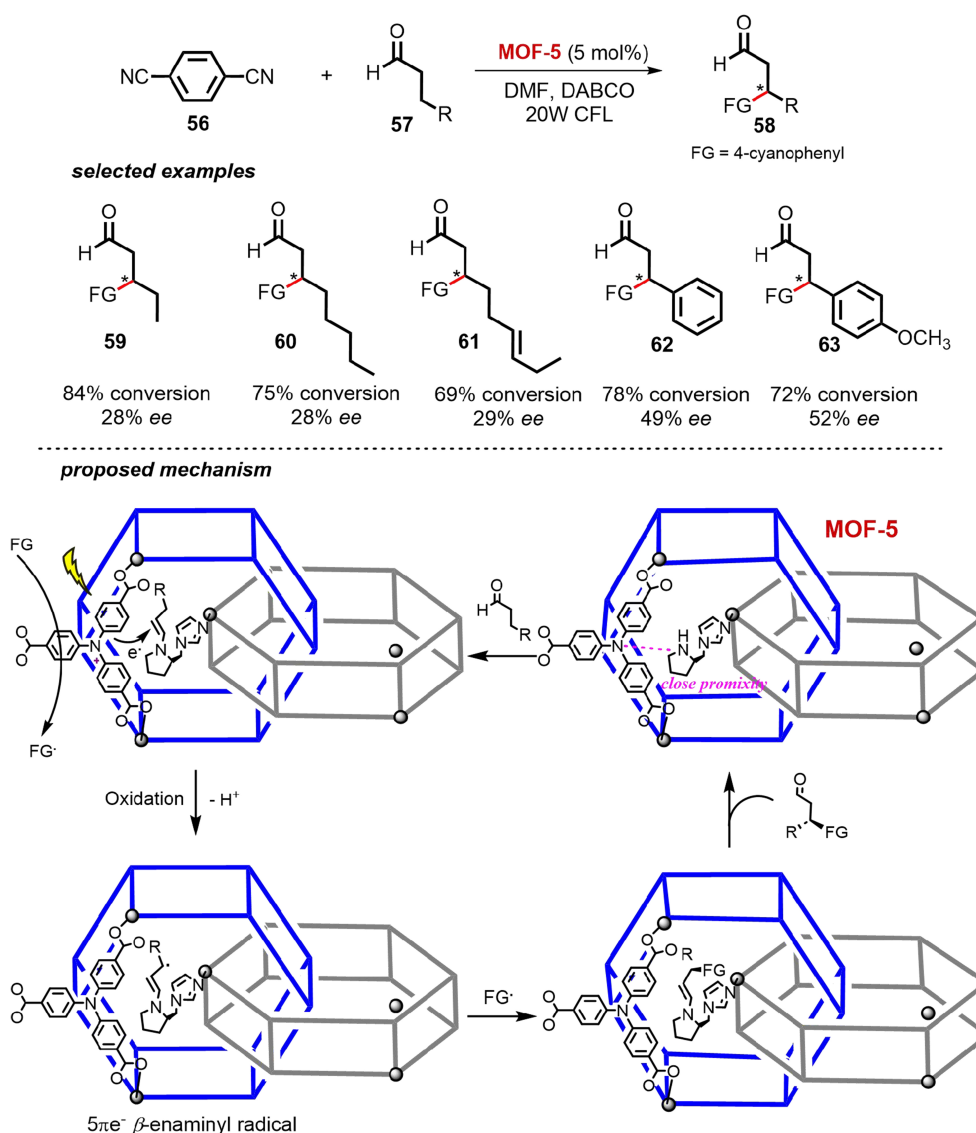


Scheme 14. Enantioselective α -alkylation of aliphatic aldehydes within Zn-based **MOF-4**. MOF: Metal-organic framework.

of MOF bearing γ -CD moieties (**MOF-3**). They demonstrated the $[4 + 4]$ photodimerization of 1-AC[−] within **MOF-3** proceeded smoothly to give the dimerization product in good yield with excellent selectivity (up to 85% yield, 91% *rr*, 79% *ee*). The solid-state superstructure indicated that stable 3D spatial configuration was constructed by four hydrogen bonds formed via 1-AC[−] anion with the four hydroxyl groups of the γ -CD (C-2 and C-3), and the hydrophobic and electrostatic interactions between carboxyl motif and four potassium cations. Two types of cavities in **MOF-3**, i.e., the $(\gamma\text{-CD})_2$ tunnels and the $(\gamma\text{-CD})_6$ cubes, play an important role during the photodimerization process. The tunnels can promote the selective transformations and the cubes can store the terminal products. The substrate 1-ACs first diffused into the $(\gamma\text{-CD})_2$ tunnels. Subsequently, two 1-AC[−] molecules reacted and the corresponding products were released into the $(\gamma\text{-CD})_6$ cubes. The multiple non-covalent bonding interactions, e.g., hydrogen bonding, π - π stacking and electrostatic interactions, result in the excellent regio- and enantioselectivity.

Asymmetric functionalization of aldehydes within MOFs

In 2012, Wu *et al.* prepared a pair of enantiomeric Zn-based MOFs (Δ/Δ -**MOF-4**) via incorporating (*L*)- or (*D*)-pyrrolidin-2-ylimidazole (PYI) and a tertiary triphenylamine redox moiety^[66]. The enantioselective α -alkylation of aldehydes could successfully take place in the confined supramolecular environment of **MOF-4** [Scheme 14]. Under the irradiation of visible light, three chiral coupling products **52** from aliphatic aldehydes **50** and diethyl 2-bromomalonate **51**, i.e., phenylpropylaldehyde **53**, octaldehyde **54** and (*E*)-non-6-ena **55**, could be obtained in good yields (74%, 65%, 84%, respectively) with excellent enantioselectivity



Scheme 15. Enantioselective β -arylation of aliphatic aldehydes with *p*-dicyanobenzene mediated by interpenetrated **MOF-5**. MOF: Metal-organic framework.

(*ee* = 92%, 86%, 92%, respectively). The results of control experiments indicated that both PYI and triphenylamine moieties were essential for the light-induced asymmetric α -alkylation reactions. The tertiary amine moiety on **MOF-4** with a strong reductive excited state initiated the photoinduced electron transfer process, producing an active intermediate for the following α -alkylation reaction. The PYI moieties served as synergistic chiral organocatalysts to promote the asymmetric catalysis. These outcomes demonstrated that MOFs can serve as a versatile platform for cooperative and tandem catalysis.

The catalytic performance of MOFs shows strong correlations with their topological structures. As shown in [Scheme 15](#), Xia *et al.* took advantage of an interpenetrated homochiral MOF (**MOF-5**) containing the photoredox and asymmetric catalytic units to achieve the enantioselective β -arylation of aldehydes (*ee* up to 52%)^[67]. X-ray single-crystal analysis showed the generation of the twofold interpenetrated coordination polymer, which shortens the space distance between two active units and, therefore, accelerates the electron

transfer between the oxidized photosensitizer and enamine intermediate. The authors postulated a possible mechanism to explain the functions of interpenetrated MOF-5 in photocatalytic β -carbonyl activation. Initially, aldehydes **57** diffused into the channels of MOF-5 and condensed with (*L*)-PYP to form the enamine intermediate. Under the irradiation of visible light, 1,4-dicyanobenzene **56** was adsorbed by MOF-5, followed by the generation of radical anion and oxidized MOF-5⁺. Subsequently, the enamine was oxidized by MOF-5⁺ through SET to form an enaminy radical cation intermediate, which increased the acidity of the allylic C–H bonds. Therefore, the deprotonation took place at the β -position of aldehyde. The $5\pi e^-$ β -enaminy radical intermediate was then coupled with a 1,4-dicyanobenzene radical anion to generate the cyclohexadienyl anion, which was hydrolyzed to the terminal β -arylation product **58** and released (*L*)-PYP to re-enter the catalytic cycle.

In the same year, Zhang *et al.* constructed a series of chiral crystalline MOFs (X-MOF-6, X = Zn, Zr, Ti) via a chiral photoredox ligand coordinated with different metal ions (Zn²⁺, Zr⁴⁺ and Ti⁴⁺), and successfully used in visible-light-induced enantioselective α -alkylation of 3-phenylpropionaldehyde and *cis*-6-nonenal [Scheme 16]^[68]. The organic ligand contains a chiral secondary amine moiety and a visible-light absorption fragment, which was formed by the condensation of chiral proline derivatives and amino-substituted terephthalic acid. This bifunctional chiral molecule only exhibited low activity in asymmetric α -alkylation of aldehydes as a homogeneous catalyst. When integrated with metal ions to form the MOFs, a significant enhancement of catalytic efficiency was recorded. Results indicated that all synthesized X-MOF-6 have excellent catalytic performances in heterogeneous α -alkylation of aldehydes. For instance, the desired α -alkylation product **52** was formed with good enantioselectivity (87% *ee*) by use of (S)-Ti-MOF under the irradiation of visible light at 0 °C. The catalytic efficiency of these MOFs could be altered with different metal ions, owing to the differences in optical absorption and charge separation among MOFs.

Other asymmetric intermolecular couplings within MOFs

MOFs can also serve as the carriers for photocatalysts or/and chiral catalysts to promote the asymmetric photochemical reactions. As shown in Scheme 17, this kind of MOF can be classified into three types based on its roles in photocatalytic asymmetric reactions: (1) chiral MOF loaded with photocatalyst (MOF-7)^[69]; (2) achiral MOF loaded with enzyme (MOF-8)^[70]; (3) supporting frameworks for photocatalyst and chiral catalyst (MOF-9, MOF-10)^[71,72]. For a clear comparison, their applications in the photocatalytic asymmetric intermolecular couplings have been summarized in Table 3.

ENANTIOSELECTIVE PHOTOREACTIONS WITHIN COFS

COFs are a class of porous and tunable crystalline polymers constructed by strong covalent bonds with 2D or 3D network topologies, which have shown great potential as heterogeneous photocatalysts^[73–78]. In general, COFs used for asymmetric photochemical reactions can be divided into two types: achiral and chiral. Achiral COFs function as supramolecular photocatalysts and are used in combination with chiral organocatalysts, while chiral COFs (CCOFs) containing both photosensitizer and chiral moieties can mediate the light-energy conversion and manipulate the stereoselectivity. This part will discuss the recent works about the designs and applications of COFs in enantioselective photochemical transformations, including α -functionalization of aldehydes, photooxidation of thioethers, and other asymmetric intermolecular couplings.

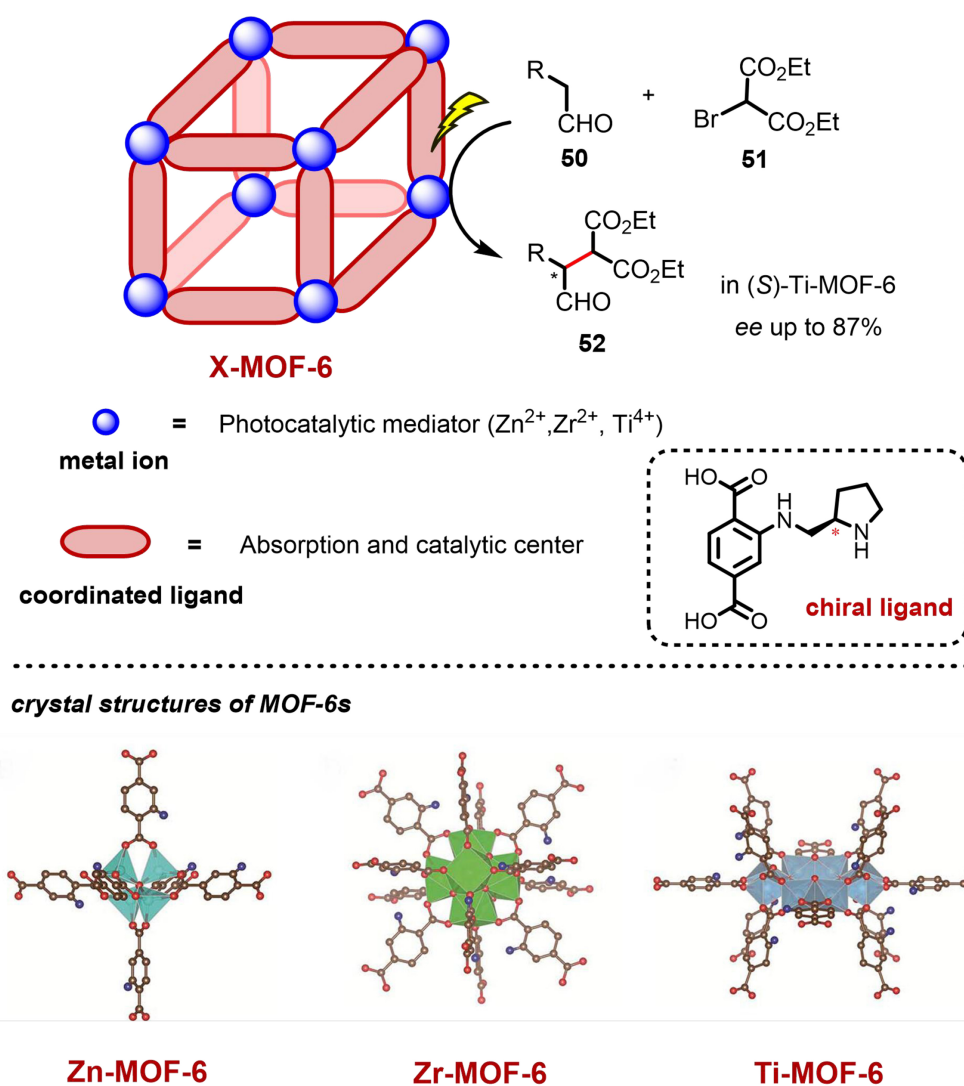
Asymmetric α -functionalization of aldehydes within COFs

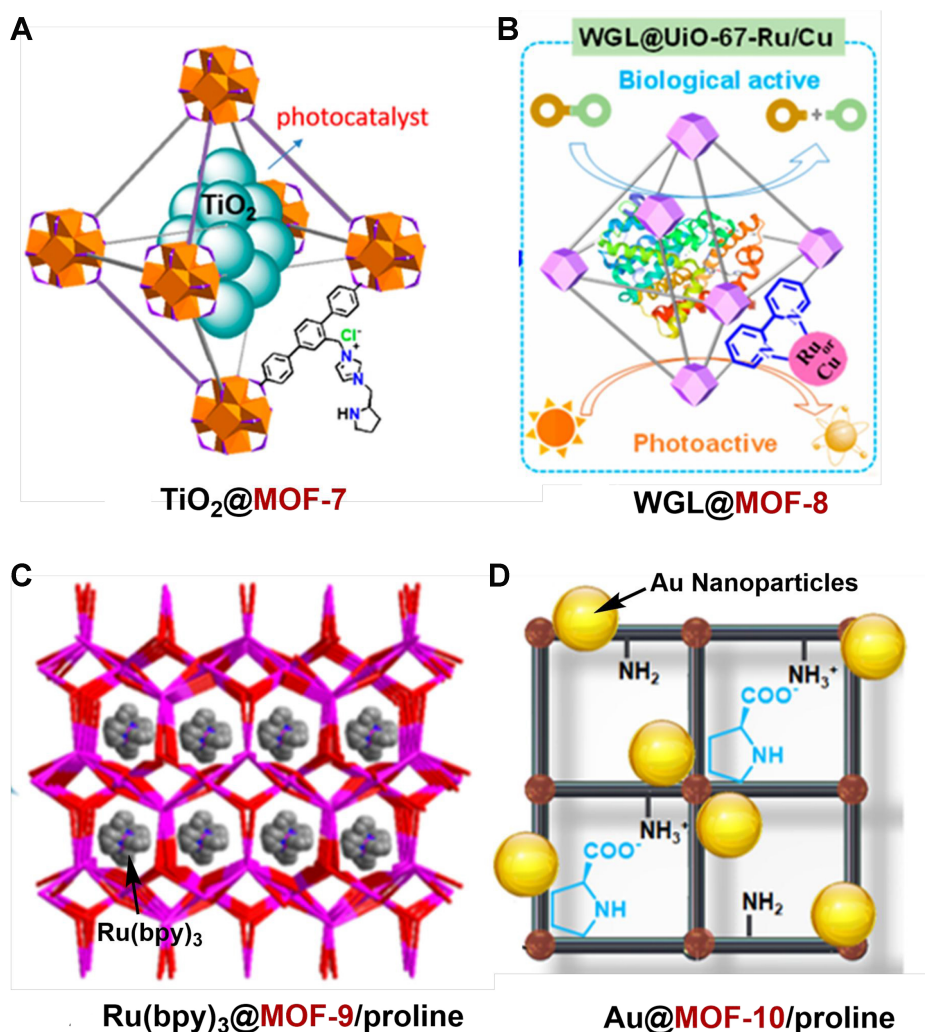
In 2020, Kang *et al.* designed a pair of 3D COFs (COF-11, COF-12) with a rare twofold-interpenetrated ffc topology through condensations between rectangular and trigonal monomers [Scheme 18]^[79]. Triphenylamine was selected as the functional molecule, since it not only exhibits unique photophysical and

Table 3. The applications of MOF carriers in photocatalytic asymmetric intermolecular couplings

MOF	Substrate	Reaction	Role	Outcome
TiO ₂ @MOF-7 ^[69]	Benzyl alcohols and methyl acrylate	Sequential MBH reaction	MOF-7: chiral induction; TiO ₂ : photocatalyst	Up to 99% yield; 99% ee
WGL@MOF-8 ^[70]	(a) Tetrahydroisoquinoline and ketones; (b) 2-arylindoles and acetone	(a) Dehydrogenation coupling; (b) Oxidative Mannich reaction	MOF-8: photocatalyst; WGL: chiral induction	Up to 65% yield; 70% ee
Ru(bpy) ₃ @MOF-9/ proline ^[71]	2-Arylindoles and ketones	Oxidative Mannich reaction	MOF-9: supporting framework; proline: chiral induction; Ru(bpy) ₃ : photocatalyst	Up to 88% yield; 99% ee
Au@MOF-10/ proline ^[72]	Aromatic aldehydes and acetone	Aldol reaction	MOF-10: supporting framework; proline: chiral induction; Au NPs: photocatalyst	Up to 81% yield; 91% ee

MOF: Metal-organic framework; MBH: Morita-Baylis-Hillman; WGL: wheat germ lipase; NPs: nanoparticles.

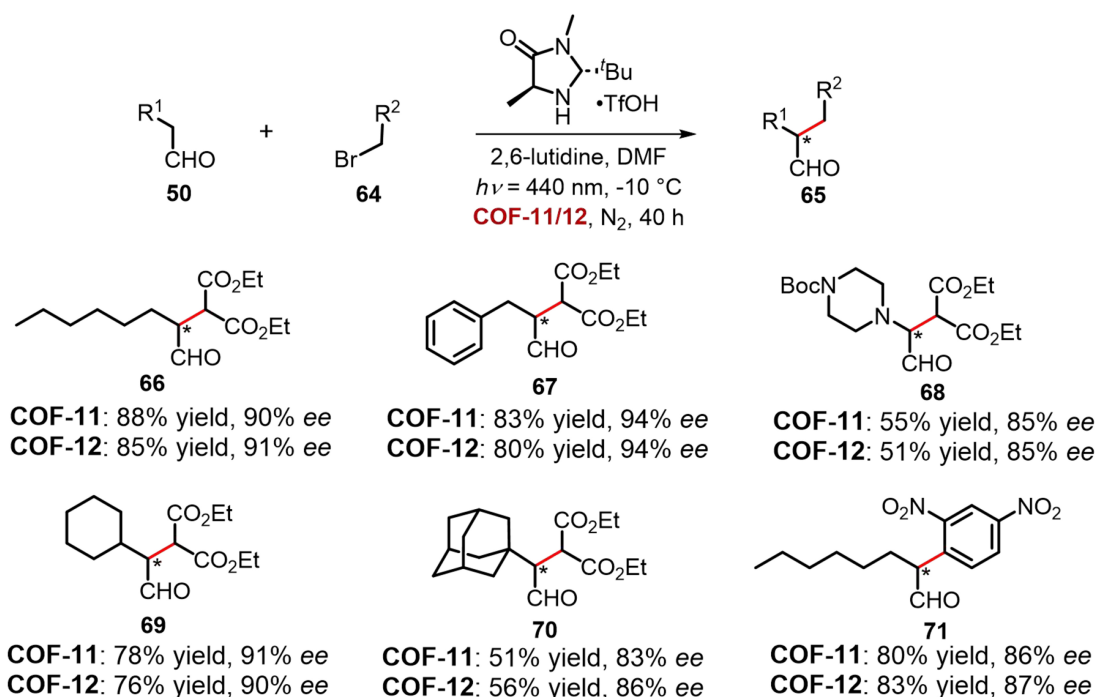
**Scheme 16.** Visible-light-mediated asymmetric α -alkylation of aldehydes within chiral **X-MOF-6**. Reproduced with permission from^[68]. Copyright 2017, American Association for the Advancement of Science. MOF: Metal-organic framework.



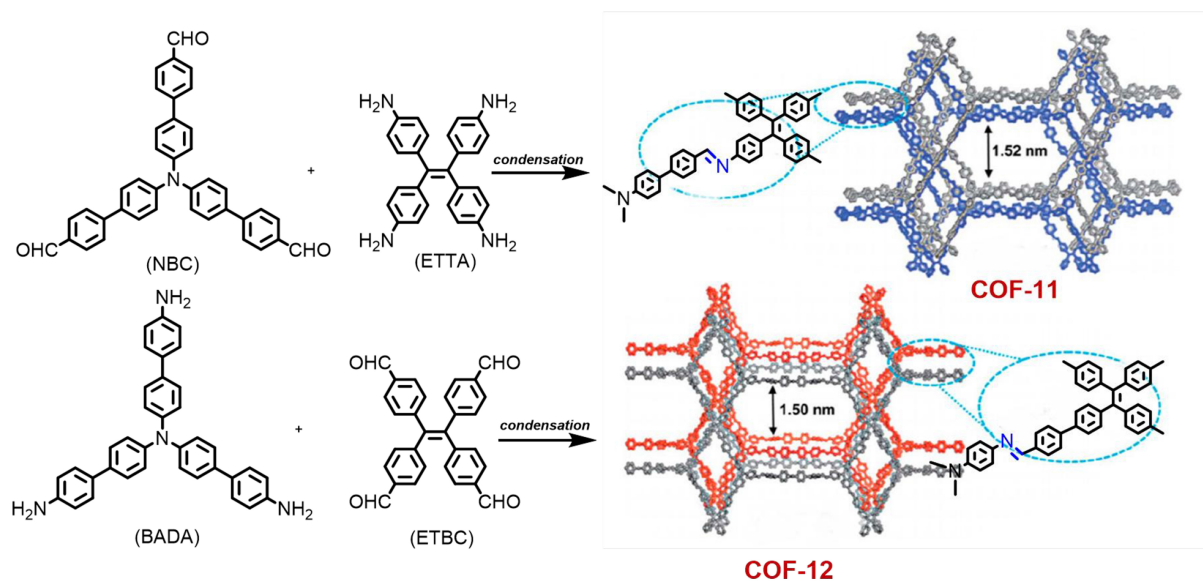
Scheme 17. MOFs loaded with photocatalyst or/and chiral catalyst employed in the photocatalytic asymmetric intermolecular couplings. (A) Reproduced with permission from^[69]. Copyright 2019, American Chemical Society; (B) Reproduced with permission from^[70]. Copyright 2024, American Chemical Society; (C) Reproduced with permission from^[71]. Copyright 2021, American Chemical Society; (D) Reproduced with permission from^[72]. Copyright 2024, Royal Society of Chemistry. MOFs: Metal-organic frameworks.

redox properties but also represents an important hole-conducting molecule. COF-11 was obtained from tetraamine (ETTA) and trialdehyde (NBC), while COF-12 was from tetraaldehyde (ETBC) and triamine (BADA). The authors proposed that both COFs adopted a twofold interpenetrated ffc topology with the $C2/m$ space after simulations. The two COFs tethered with a chiral amine organocatalyst could catalyze the asymmetric α -alkylation of aldehydes, which exhibited similar catalytic performances in reactivity and enantioselectivity. Under the optimized conditions, the desired α -alkylation products **65** were formed in good yields with excellent enantioselectivity (up to 88% yield, 94% *ee*).

Li *et al.* also synthesized two robust tetrahydroquinoline-linked (QH)-COFs (COF-13, COF-14) visible light photocatalysts and used in the enantioselective photochemical α -alkylation of aldehydes [Scheme 19]^[80]. The tetrahydroquinoline linkage plays an important role in enhancing the stability and widening the absorption spectrum of COFs. Up to 94% *ee* was obtained using this kind of COF by merging with a chiral secondary amine, and the catalytic efficiency is similar to that of conventional Ru catalyst $[Ru(bpy)_3]Cl_2 \cdot 6H_2O$ (80%

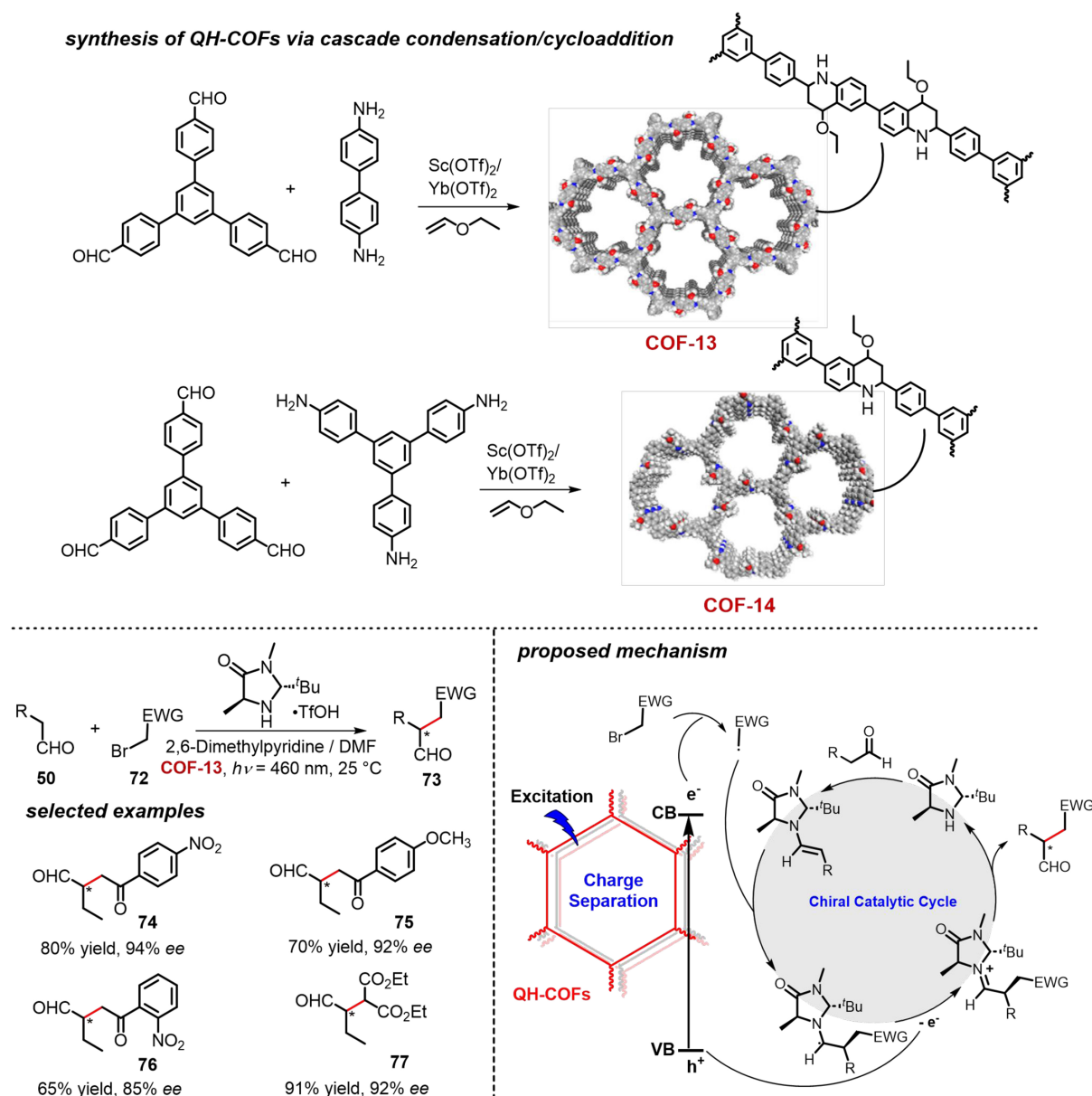


twofold interpenetrated ffc network of 3D COFs



Scheme 18. Highly enantioselective α -alkylation of aldehydes within 3D COFs. Reproduced with permission from [79]. Copyright 2020, Royal Society of Chemistry. COFs: Covalent organic frameworks.

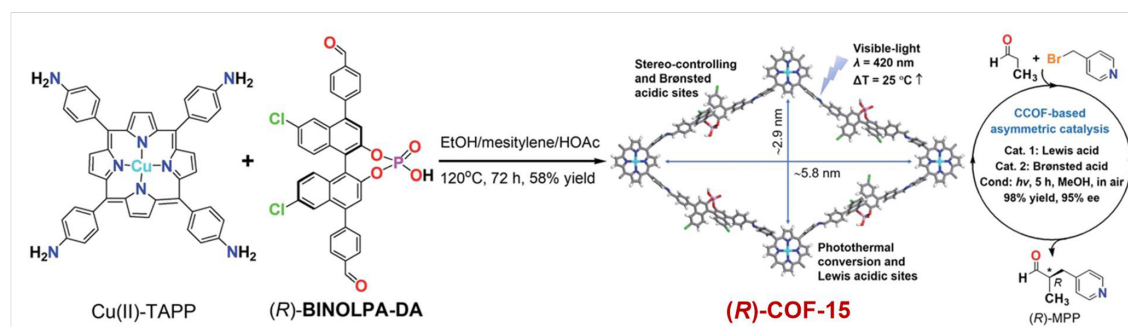
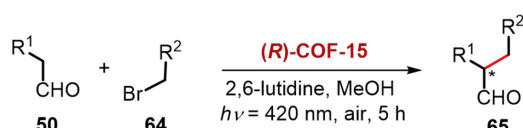
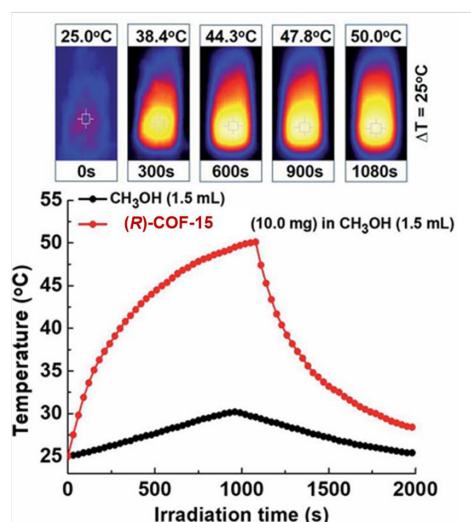
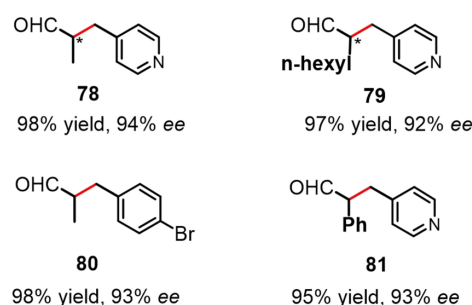
yield, 91% ee). In this study, the authors also proposed a possible catalytic mechanism. Under visible light irradiation, one electron was transferred from the conduction band (CB) of COFs to α -bromocarbonyl substrate 72, thus leading to the formation of the alkyl radical intermediate. Then, aldehyde 50 condensed with the chiral secondary amine organic catalyst to form an enamine intermediate, followed by the addition of the electron-deficient alkyl radical. Subsequently, the generated α -amino radical delivered one electron to the hole in the VB of QH-COFs and formed an imine cation. Hydrolysis of the imine intermediate afforded



Scheme 19. Visible-light-induced enantioselective α -alkylation of aldehydes within QH-COFs merging with a chiral secondary amine. Reproduced with permission from [80]. Copyright 2020, Elsevier. QH-COFs: Tetrahydroquinoline-linked covalent organic frameworks.

the terminal product and regenerated the catalyst to finish the cycle. Additionally, Zhou *et al.* also synthesized an achiral photoactive COF by the condensation of 1,3,6,8-tetrakis(4-formylphenyl) pyrene with amino/cyano-containing monomers. By merging with a chiral amine catalyst, the asymmetric α -alkylation of aldehydes proceeded quite well under visible light irradiation [81].

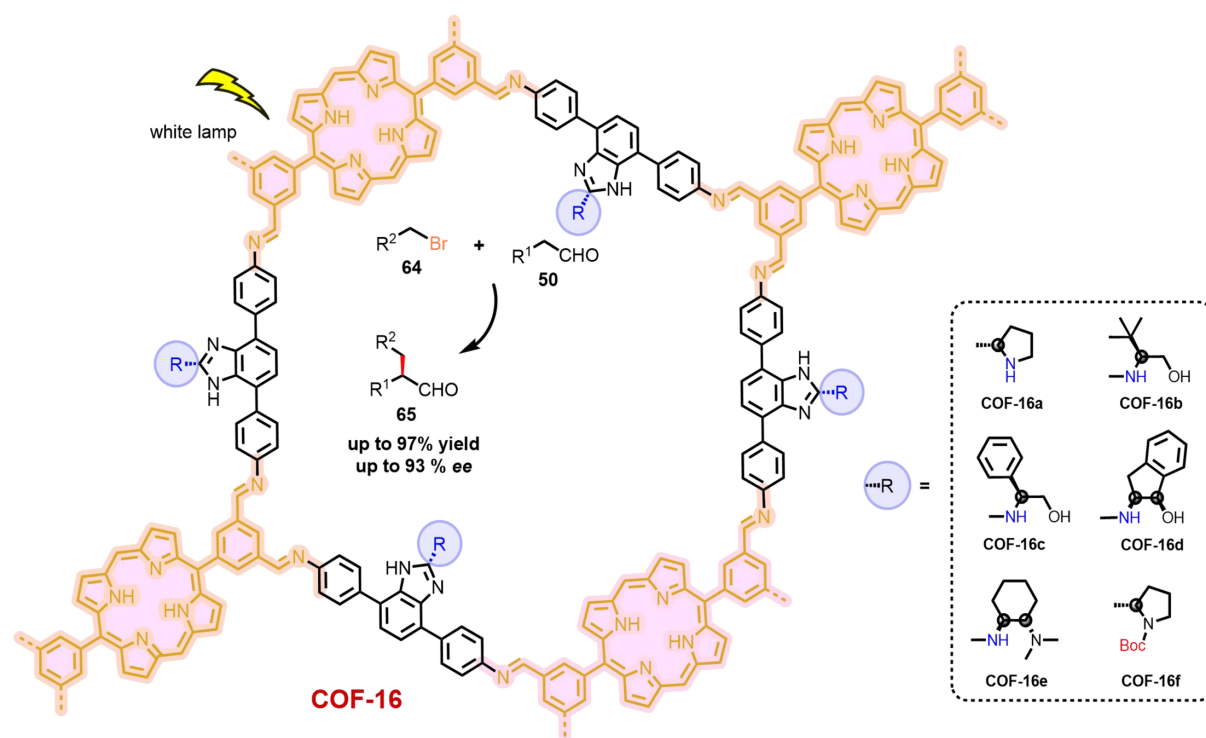
Regarding asymmetric photochemical reactions, achiral COFs usually served as photocatalysts to harvest light and chiral induction usually required an additional chiral catalyst. The construction of CCOFs by merging photoactive and chiral units into a single framework is a promising strategy. In 2022, Ma *et al.* designed and synthesized a chiral multifunctional COF (COF-15) through the condensation of chiral BINOL-phosphate with Cu(II)-porphyrin-derived monomers, and successfully introduced in the

synthesis of (R)-COF-15 combining chiral BINOL-phosphate and Cu(II)-porphyrin derivatives**photothermal behaviour of (R)-COF-15 in MeOH****selected examples**

Scheme 20. Photoinduced thermally-driven enantioselective α-benylation of aldehydes catalyzed by (R)-COF-15. Reproduced with permission from [82]. Copyright 2022, Royal Society of Chemistry. COF: Covalent organic framework.

enantioselective α-benylation of aldehydes [Scheme 20]^[82]. COF-15 bears both Brønsted (phosphate) and Lewis [Cu(II)] acidic catalytic sites, chiral confinement space, and photothermal conversion (PTC) properties. Upon 420 nm light irradiation, (R)-COF-15 could catalyze the α-benylation of aldehydes with alkyl halides in good yields with excellent enantioselectivity (ten examples, up to 98% yields, 94% *ees*). The PTC behavior of COF-15 was also investigated, and results indicated that a significant temperature increase was observed when a solution of (R)-COF-15 in MeOH was irradiated under 420 nm light for 18 min. Interestingly, the configuration of the terminal product could be easily reversed by tuning the chirality of MOF, without any loss of yield and *ee*.

Recently, He *et al.* has successfully synthesized a series of CCOFs (COF-16a-16f) with photoactive porphyrin moieties as knots, and secondary-amine-based chiral functional groups were fixed on the benzoimidazole linkers [Scheme 21]^[83]. Among these CCOF photocatalysts, COF-16a exhibited the best results in the enantioselective α-alkylation of aldehydes 50 in high yields (up to 97%) with good enantioselectivity (up to 93% *ee*) under visible light irradiation. The good results benefited from the activation of bromide 64 by porphyrin units and aldehydes by chiral secondary amines. The authors also investigated the physical and chemical properties of these COFs. Broad absorption region and excellent stability and recyclability also showed their advantages as metal-free catalytic platforms in enantioselective



Scheme 21. Visible-light-mediated enantioselective α -alkylation of aldehydes catalyzed by **COF-16**. COF: Covalent organic framework.

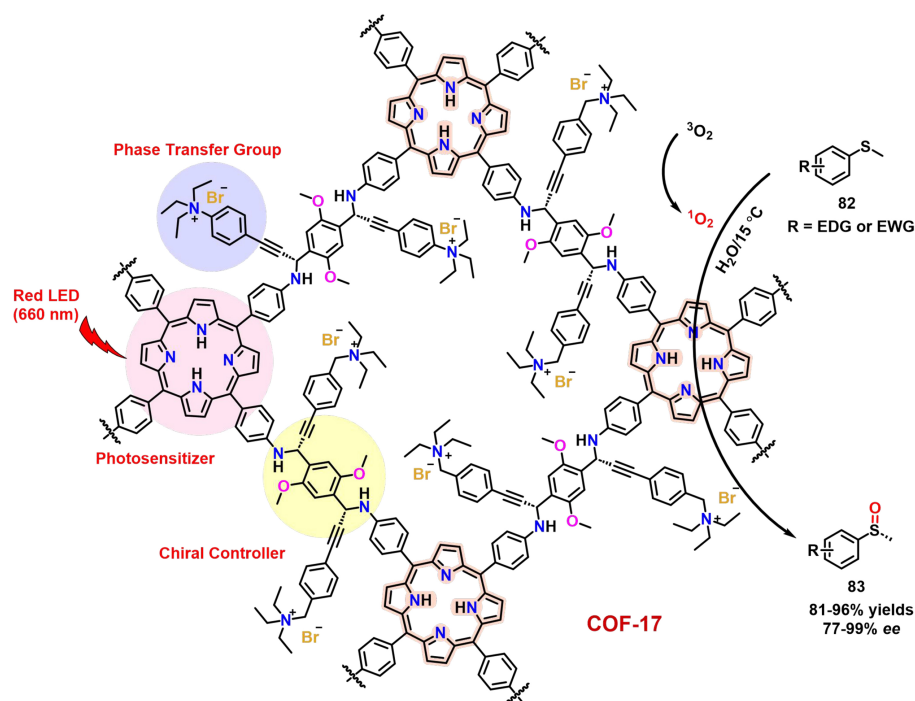
photocatalysis.

Asymmetric photooxidation within COFs

In 2022, Kan *et al.* designed and constructed a photoactive and hydrotropic CCOF (**COF-17**) bearing a photosensitizer, chiral moiety, phase transfer group and linkage, which was successfully applied in the enantioselective photooxidation of sulfides to sulfoxides in water [Scheme 22]^[84]. This homochiral **COF-17** was synthesized via asymmetric A^3 -coupling polymerization of 2,5-dimethoxyterephthalaldehyde, quaternary ammonium bromide-modified phenylacetylene and 5,10,15,20-tetrakis(4-aminophenyl)porphyrin. The key active units, photosensitive porphyrin, chiral propargylamine linkage and amphipathic quaternary ammonium bromide, were introduced into the CCOF supramolecular catalyst. Under the irradiation of 660 nm light, (*R*)-**COF-17** could catalyze the oxidation of substituted methylphenylsulfides **82** to the corresponding (*R*)-methylphenylsulfoxides **83** in water with molecular oxygen in air as the oxidant (81%-96% yields, 77%-99% *ee*). Interestingly, biologically active (*R*)-modafinil could also be obtained using this protocol.

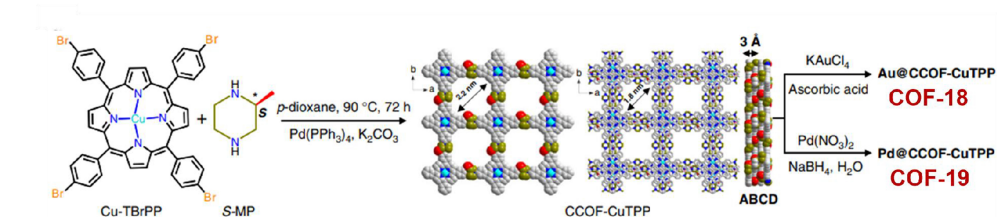
Other asymmetric intermolecular couplings within COFs

Photoactive CCOFs integrated with metal nanoparticles (M NPs) are also suitable for enantioselective photochemical reactions. For instance, Ma *et al.* designed two kinds of M NP (M = Au, Pd)-loaded and Cu(II)-porphyrin-containing homochiral COFs (**COF-18**, **COF-19**), which exhibited excellent PTC and asymmetric catalytic performance in visible-light-induced thermally-driven enantioselective Henry and A^3 -coupling [Scheme 23]^[85]. For instance, Henry reaction between benzylic alcohols **84** and nitromethane **85** within **COF-18** could generate the desired nitroaldols **86** in high yields (up to 99%) with excellent enantioselectivity (*ee* of up to 98%). Meanwhile, A^3 -coupling of benzaldehyde derivatives **87**, aromatic alkynes **88** and secondary amines **89** within **COF-19** also took place and delivered the products in good results (yield of up to 98%, *ee* of up to 98%). According to the experimental results, the loading of M NPs



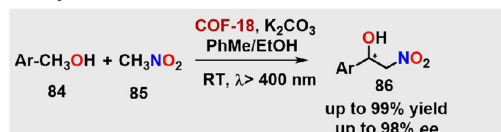
Scheme 22. Enantioselective aerobic photooxidation of sulfides into sulfoxides catalyzed by **COF-17**. COF: Covalent organic framework.

synthesis of Au NP-loaded COF-18 and Pd NP-loaded COF-19

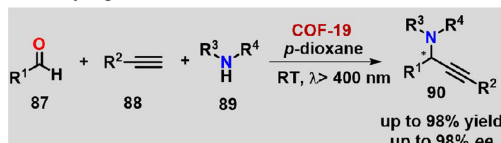


COF-18/19 catalyzed Henry and A³-coupling reactions

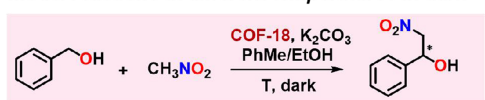
- Henry reaction



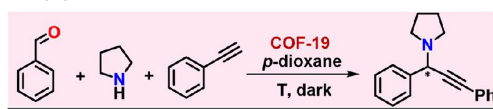
- A³-coupling reaction



model reactions at different temperatures in dark

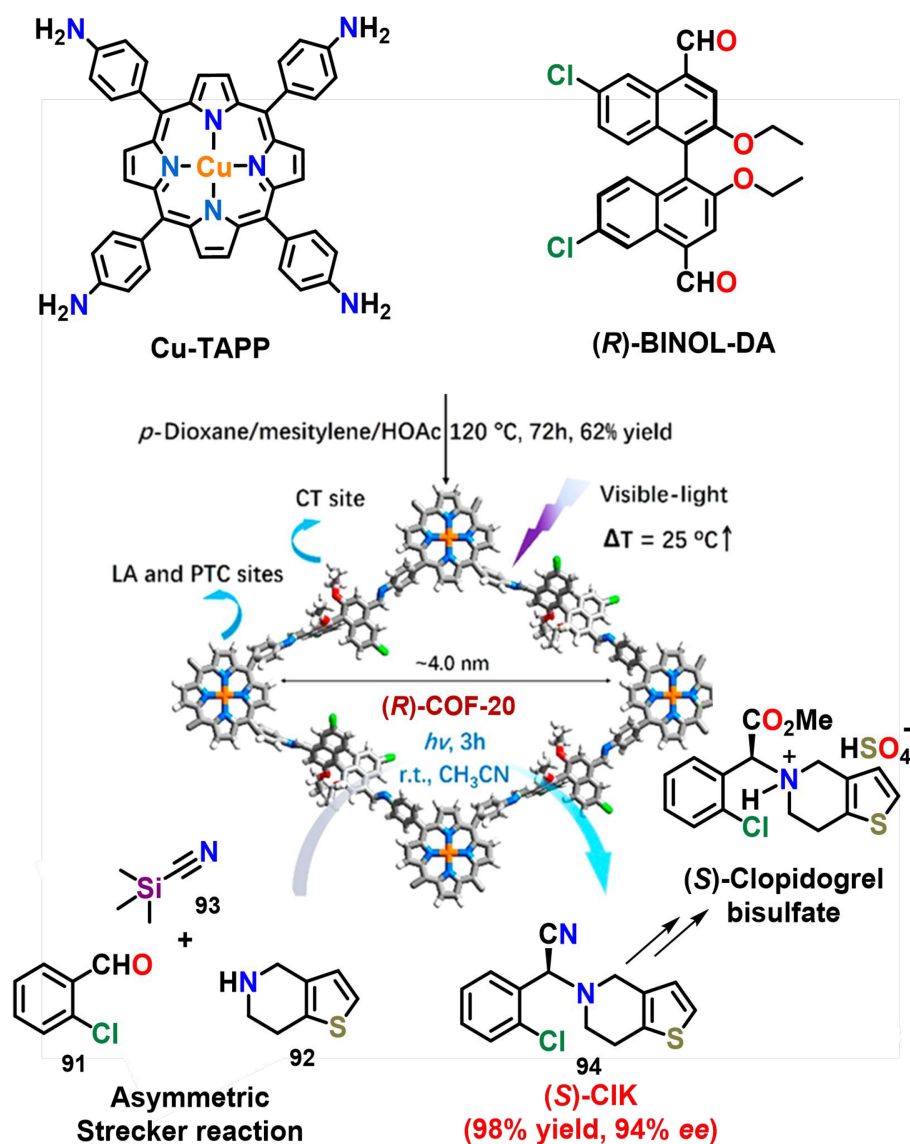


T (°C)	60	70	80	90	100
Yield (%)	97	97	98	98	99
ee (%)	96	97	95	93	88



T (°C)	60	70	80	90	100
Yield (%)	97	97	98	98	99
ee (%)	97	96	96	92	86

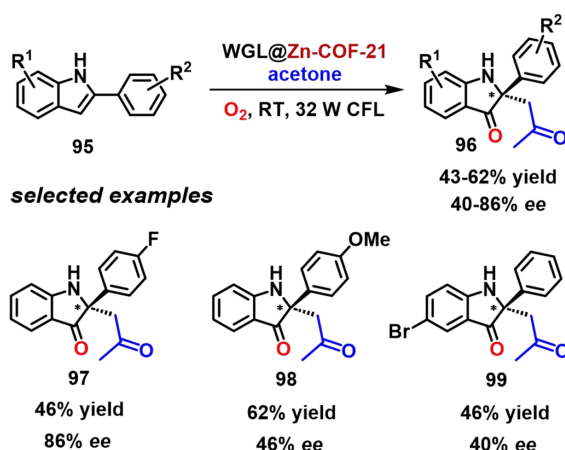
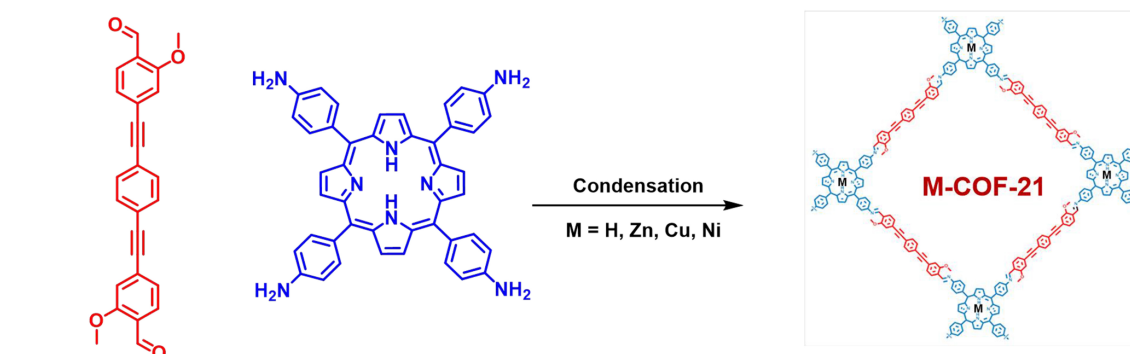
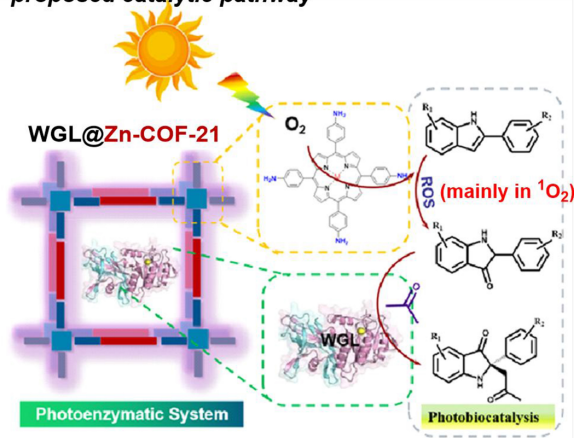
Scheme 23. Asymmetric visible-light-induced thermally-driven Henry and A³-coupling reactions within chiral COFs loaded with metal nanoparticles. Reproduced with permission from [85]. Copyright 2019, Springer Nature. COFs: Covalent organic frameworks.



Scheme 24. Visible-light-induced asymmetric synthesis of drug intermediate (S)-CIK catalyzed by **COF-20**. Reproduced with permission from [86]. Copyright 2020, American Chemical Society. COF: Covalent organic framework.

into COFs would not affect the PTC efficiency. The confinement of CCOFs played a crucial role in suppressing the racemization of the terminal products under high temperatures.

Ma *et al.* employed a versatile homochiral COF (**COF-20**) synthesized by the condensation of Cu(II)-porphyrin-derived monomers [5,10,15,20-tetrakis(4-aminophenyl)porphyrin-Cu-(II) (**Cu-TAPP**)] and chiral (*R*)-4,4'-dialdehyde-6,6'-dichloro-2,2'-diethoxy-1,1'-binaphthalene [(*R*)-**BINOL-DA**] [86]. **COF-20** possessed multiple active sites, including chiral templating (CT), Lewis acid (LA) and PTC sites, which ensured its excellent performance in catalyzing the asymmetric Strecker reaction (98% yield, 94% ee). They successfully used **COF-20** to synthesize the (S)-**CIK 94**, a key intermediate in the synthesis of antithrombotic drug (S)-clonidogrel [Scheme 24]. The detailed physical and chemical property studies of **COF-20** were also conducted. This study further demonstrated the promising potential of CCOFs as a green and facile synthesis platform for chiral drug preparation and discovery.

synthesis of M-COF-21**proposed catalytic pathway**

Scheme 25. Asymmetric oxidative Mannich reaction catalyzed by a heterogeneous photobiocatalyst WGL@M-COF-21. Reproduced with permission from [87]. Copyright 2022, American Chemical Society. WGL: Wheat germ lipase; COF: covalent organic framework.

In the last few years, the combination of photocatalysis and biocatalysis has attracted much research interest in asymmetric synthesis. Merging photoactive COFs with enzymatic catalysts is an effective strategy to promote enantioselective photochemical reactions. Recently, Jin *et al.* developed a COF-based photoenzymatic platform for asymmetric oxidative Mannich reaction [Scheme 25]^[87]. In this study, a photoactive M-porphyrin-containing COF (M-COF-21; M = H, Zn, Cu, Ni) served as a porous carrier to encapsulate wheat germ lipase (WGL) and generated a heterogeneous photobiocatalyst (WGL@M-COF-21). This catalyst could promote the sequential oxidation and asymmetric Mannich reaction of 2-arylidole derivatives **95** under visible-light irradiation with O₂ as the oxidant and acetone as the nucleophile. Based on the mechanism studies, the authors proposed a possible catalytic pathway in which photoactive M-COF-21 oxidized the substrate using the generated reactive oxygen species (ROS), and then WGL catalyzed the following Mannich reaction to produce the desired products **96** in moderate yields with moderate to good enantioselectivity (ten examples, 43%-62% yields, 40%-86% *ees*).

CONCLUSION AND OUTLOOK

In the review, we have summarized the recent advances in enantioselective photochemical reactions within the confined spaces of supramolecular assemblies including macrocycles, MOCs, MOFs, and COFs. This research field has flourished over the past two decades, accompanied with the development of new types of supramolecular hosts with excellent catalytic and stereo-controlled performance. However, there are still some limitations in supramolecular enantioselective photocatalysis. For instance: (1) The types of chiral

hosts for enantioselective photochemical reactions are not diverse. Macrocycles are largely limited to CDs, and chiral organocatalysts immobilized into MOFs and COFs are mainly based on chiral secondary amines and BINOL backbones; (2) The reaction types are quite narrow. CDs-initiated reactions are mainly focused on photodimerization of 2-ACs. Most of the asymmetric reactions mediated by MOCs, MOFs and COFs are [2 + 2] photocycloaddition reactions and α -alkylation of aldehydes; (3) Only a few guest molecules can be accommodated very well in the rigid cavities of chiral hosts, leading to the low substrate diversities.

To enrich the library of chiral hosts for enantioselective photochemical reactions, other modified metal complexes and organic photosensitizers could be used to construct new types of chiral supramolecular hosts. Meanwhile, some other chiral privileged structures, e.g., chiral hydrogen bonding moieties (urea, thiourea), *N*-heterocyclic carbenes and chiral tertiary amines, can be incorporated into the hosts, or as cooperative catalysts in supramolecular enantioselective photochemical reactions. By doing so, growing reaction substrates can be introduced, and therefore, the reaction types could be further expanded. On the other hand, dual activation models by the combination of supramolecular catalysis with transition metal or LA catalysis are also potential strategies. Future advances can be expected along these lines.

DECLARATIONS

Acknowledgments

We thank M.Sc. Xiao-Yu He (Wuhan University) for the helpful discussions and for proofreading the final version of this manuscript. We also express our gratitude to all leading chemists and co-workers involved in the development of enantioselective supramolecular photocatalysis.

Authors' contributions

Wrote the draft manuscript: Su YW, Pan C, Sun TY

Initiated and supervised the work, and revised the manuscript: Zou YQ

Availability of data and materials

Not applicable.

Financial support and sponsorship

Financial support by the start-up funding from Wuhan University (Nos. 691000002 and 600460026) and Taikang Center for Life and Medical Sciences (No. 692000007) is gratefully acknowledged.

Conflicts of interest

All authors declared that there are no conflicts of interest.

Ethical approval and consent to participate

Not applicable.

Consent for publication

Not applicable.

Copyright

© The Author(s) 2024.

REFERENCES

1. Brimiouille, R.; Lenhart, D.; Maturi, M. M.; Bach, T. Enantioselective catalysis of photochemical reactions. *Angew. Chem. Int. Ed. Engl.* **2015**, *54*, 3872-90. DOI [PubMed](#)

2. Yao, W.; Bergamino, E. A. B.; Ngai, M. Y. Asymmetric photocatalysis enabled by chiral organocatalysts. *ChemCatChem* **2022**, *14*, e202101292. DOI PubMed PMC
3. Jiang, C.; Chen, W.; Zheng, W. H.; Lu, H. Advances in asymmetric visible-light photocatalysis, 2015-2019. *Org. Biomol. Chem.* **2019**, *17*, 8673-89. DOI PubMed
4. Zarra, S.; Wood, D. M.; Roberts, D. A.; Nitschke, J. R. Molecular containers in complex chemical systems. *Chem. Soc. Rev.* **2015**, *44*, 419-32. DOI PubMed
5. Morimoto, M.; Bierschenk, S. M.; Xia, K. T.; Bergman, R. G.; Raymond, K. N.; Toste, F. D. Advances in supramolecular host-mediated reactivity. *Nat. Catal.* **2020**, *3*, 969-84. DOI
6. Ramamurthy, V.; Gupta, S. Supramolecular photochemistry: from molecular crystals to water-soluble capsules. *Chem. Soc. Rev.* **2015**, *44*, 119-35. DOI PubMed
7. Ramamurthy, V.; Sivaguru, J. Supramolecular photochemistry as a potential synthetic tool: photocycloaddition. *Chem. Rev.* **2016**, *116*, 9914-93. DOI PubMed
8. Gao, W.; Zhang, H.; Jin, G. Supramolecular catalysis based on discrete heterometallic coordination-driven metallacycles and metallacages. *Coordin. Chem. Rev.* **2019**, *386*, 69-84. DOI
9. Liu, Y.; Xuan, W.; Cui, Y. Engineering homochiral metal-organic frameworks for heterogeneous asymmetric catalysis and enantioselective separation. *Adv. Mater.* **2010**, *22*, 4112-35. DOI PubMed
10. Hao, Y.; Lu, Y. L.; Jiao, Z.; Su, C. Y. Photocatalysis meets confinement: an emerging opportunity for photoinduced organic transformations. *Angew. Chem. Int. Ed. Engl.* **2024**, *63*, e202317808. DOI PubMed
11. Ballester, P.; Wang, Q. Q.; Gaeta, C. Supramolecular approaches to mediate chemical reactivity. *Beilstein. J. Org. Chem.* **2022**, *18*, 1463-5. DOI PubMed PMC
12. Ham, R.; Nielsen, C. J.; Pullen, S.; Reek, J. N. H. Supramolecular coordination cages for artificial photosynthesis and synthetic photocatalysis. *Chem. Rev.* **2023**, *123*, 5225-61. DOI PubMed PMC
13. Olivo, G.; Capocasa, G.; Del, G. D.; Lanzalunga, O.; Di, S. S. New horizons for catalysis disclosed by supramolecular chemistry. *Chem. Soc. Rev.* **2021**, *50*, 7681-724. DOI PubMed
14. Meeuwissen, J.; Reek, J. N. Supramolecular catalysis beyond enzyme mimics. *Nat. Chem.* **2010**, *2*, 615-21. DOI PubMed
15. Hong, C. M.; Bergman, R. G.; Raymond, K. N.; Toste, F. D. Self-assembled tetrahedral hosts as supramolecular catalysts. *Acc. Chem. Res.* **2018**, *51*, 2447-55. DOI PubMed
16. Jing, X.; He, C.; Zhao, L.; Duan, C. Photochemical properties of host-guest supramolecular systems with structurally confined metal-organic capsules. *Acc. Chem. Res.* **2019**, *52*, 100-9. DOI PubMed
17. Pascanu, V.; González, M. G.; Inge, A. K.; Martín-Matute, B. Metal-organic frameworks as catalysts for organic synthesis: a critical perspective. *J. Am. Chem. Soc.* **2019**, *141*, 7223-34. DOI PubMed
18. Zhang, Q.; Catti, L.; Tiefenbacher, K. Catalysis inside the hexameric resorcinarene capsule. *Acc. Chem. Res.* **2018**, *51*, 2107-14. DOI PubMed
19. Wang, M. X. Nitrogen and oxygen bridged calixaromatics: synthesis, structure, functionalization, and molecular recognition. *Acc. Chem. Res.* **2012**, *45*, 182-95. DOI PubMed
20. Fang, Y.; Powell, J. A.; Li, E.; et al. Catalytic reactions within the cavity of coordination cages. *Chem. Soc. Rev.* **2019**, *48*, 4707-30. DOI PubMed
21. Qin, B.; Yin, Z.; Tang, X.; et al. Supramolecular polymer chemistry: from structural control to functional assembly. *Prog. Polym. Sci.* **2020**, *100*, 101167. DOI
22. Vallavoju, N.; Sivaguru, J. Supramolecular photocatalysis: combining confinement and non-covalent interactions to control light initiated reactions. *Chem. Soc. Rev.* **2014**, *43*, 4084-101. DOI PubMed
23. Yang, C.; Inoue, Y. Supramolecular photochirogenesis. *Chem. Soc. Rev.* **2014**, *43*, 4123-43. DOI PubMed
24. Nishijima, M.; Wada, T.; Mori, T.; Pace, T. C.; Bohne, C.; Inoue, Y. Highly enantiomeric supramolecular [4 + 4] photocyclodimerization of 2-anthracenecarboxylate mediated by human serum albumin. *J. Am. Chem. Soc.* **2007**, *129*, 3478-9. DOI PubMed
25. Wada, T.; Nishijima, M.; Fujisawa, T.; et al. Bovine serum albumin-mediated enantiodifferentiating photocyclodimerization of 2-anthracenecarboxylate. *J. Am. Chem. Soc.* **2003**, *125*, 7492-3. DOI PubMed
26. Ishida, Y.; Kai, Y.; Kato, S. Y.; et al. Two-component liquid crystals as chiral reaction media: highly enantioselective photodimerization of an anthracene derivative driven by the ordered microenvironment. *Angew. Chem. Int. Ed. Engl.* **2008**, *47*, 8241-5. DOI PubMed
27. Ishida, Y.; Matsuoka, Y.; Kai, Y.; et al. Metastable liquid crystal as time-responsive reaction medium: aging-induced dual enantioselective control. *J. Am. Chem. Soc.* **2013**, *135*, 6407-10. DOI PubMed
28. Ji, J.; Wei, X.; Wu, W.; Yang, C. Asymmetric photoreactions in supramolecular assemblies. *Acc. Chem. Res.* **2023**, *56*, 1896-907. DOI PubMed
29. Wei, X.; Wu, W.; Matsushita, R.; et al. Supramolecular photochirogenesis driven by higher-order complexation: enantiodifferentiating photocyclodimerization of 2-anthracenecarboxylate to slipped cyclodimers via a 2:2 complex with β -cyclodextrin. *J. Am. Chem. Soc.* **2018**, *140*, 3959-74. DOI PubMed
30. Rekharsky, M. V.; Inoue, Y. Complexation thermodynamics of cyclodextrins. *Chem. Rev.* **1998**, *98*, 1875-918. DOI PubMed
31. Nakamura, A.; Inoue, Y. Supramolecular catalysis of the enantiodifferentiating [4 + 4] photocyclodimerization of 2-

- anthracenecarboxylate by gamma-cyclodextrin. *J. Am. Chem. Soc.* **2003**, *125*, 966-72. DOI PubMed
32. Nakamura, A.; Inoue, Y. Electrostatic manipulation of enantiodifferentiating photocyclodimerization of 2-anthracenecarboxylate within gamma-cyclodextrin cavity through chemical modification. inverted product distribution and enhanced enantioselectivity. *J. Am. Chem. Soc.* **2005**, *127*, 5338-9. DOI PubMed
33. Yang, C.; Nakamura, A.; Wada, T.; Inoue, Y. Enantiodifferentiating photocyclodimerization of 2-anthracenecarboxylic acid mediated by gamma-cyclodextrins with a flexible or rigid cap. *Org. Lett.* **2006**, *8*, 3005-8. DOI PubMed
34. Yang, C.; Mori, T.; Origane, Y.; et al. Highly stereoselective photocyclodimerization of alpha-cyclodextrin-appended anthracene mediated by gamma-cyclodextrin and cucurbit[8]uril: a dramatic steric effect operating outside the binding site. *J. Am. Chem. Soc.* **2008**, *130*, 8574-5. DOI PubMed
35. Ke, C.; Yang, C.; Mori, T.; Wada, T.; Liu, Y.; Inoue, Y. Catalytic enantiodifferentiating photocyclodimerization of 2-anthracenecarboxylic acid mediated by a non-sensitizing chiral metallosupramolecular host. *Angew. Chem. Int. Ed. Engl.* **2009**, *48*, 6675-7. DOI PubMed
36. Luo, L.; Liao, G. H.; Wu, X. L.; Lei, L.; Tung, C. H.; Wu, L. Z. Gamma-cyclodextrin-directed enantioselective photocyclodimerization of methyl 3-methoxyl-2-naphthoate. *J. Org. Chem.* **2009**, *74*, 3506-15. DOI PubMed
37. Yang, C.; Ke, C.; Liang, W.; et al. Dual supramolecular photochirogenesis: ultimate stereocontrol of photocyclodimerization by a chiral scaffold and confining host. *J. Am. Chem. Soc.* **2011**, *133*, 13786-9. DOI PubMed
38. Yao, J.; Yan, Z.; Ji, J.; et al. Ammonia-driven chirality inversion and enhancement in enantiodifferentiating photocyclodimerization of 2-anthracenecarboxylate mediated by diguanidino- γ -cyclodextrin. *J. Am. Chem. Soc.* **2014**, *136*, 6916-9. DOI PubMed
39. Ji, J.; Wu, W.; Liang, W.; et al. An ultimate stereocontrol in supramolecular photochirogenesis: photocyclodimerization of 2-anthracenecarboxylate mediated by sulfur-linked β -cyclodextrin dimers. *J. Am. Chem. Soc.* **2019**, *141*, 9225-38. DOI PubMed
40. Kanagaraj, K.; Liang, W.; Rao, M.; et al. pH-controlled chirality inversion in enantiodifferentiating photocyclodimerization of 2-anthracenecarboxylic acid mediated by γ -cyclodextrin derivatives. *Org. Lett.* **2020**, *22*, 5273-8. DOI PubMed
41. Wei, X.; Raj, A. M.; Ji, J.; et al. Reversal of regioselectivity during photodimerization of 2-anthracenecarboxylic acid in a water-soluble organic cavitand. *Org. Lett.* **2019**, *21*, 7868-72. DOI PubMed
42. Rau, H. Asymmetric photochemistry in solution. *Chem. Rev.* **1983**, *83*, 535-47. DOI
43. Inoue, Y. Asymmetric photochemical reactions in solution. *Chem. Rev.* **1992**, *92*, 741-70. DOI
44. Genzink, M. J.; Kidd, J. B.; Swords, W. B.; Yoon, T. P. Chiral photocatalyst structures in asymmetric photochemical synthesis. *Chem. Rev.* **2022**, *122*, 1654-716. DOI PubMed PMC
45. Koodanjeri, S.; Joy, A.; Ramamurthy, V. Asymmetric induction with cyclodextrins: photocyclization of tropolone alkyl ethers. *Tetrahedron* **2000**, *56*, 7003-9. DOI
46. Shailaja, J.; Karthikeyan, S.; Ramamurthy, V. Cyclodextrin mediated solvent-free enantioselective photocyclization of N-alkyl pyridones. *Tetrahedron. Lett.* **2002**, *43*, 9335-9. DOI
47. Kaliappan, R.; Ramamurthy, V. Chiral photochemistry within natural and functionalized cyclodextrins: chiral induction in photocyclization products from carbonyl compounds. *J. Photoch. Photobio. A.* **2009**, *207*, 144-52. DOI
48. Mansour, A. T.; Buendia, J.; Xie, J.; et al. β -cyclodextrin-mediated enantioselective photochemical electrocycloization of 1,3-dihydro-2H-azepin-2-one. *J. Org. Chem.* **2017**, *82*, 9832-6. DOI PubMed
49. Fukuhara, G.; Mori, T.; Inoue, Y. The first supramolecular photosensitization of enantiodifferentiating bimolecular reaction: anti-Markovnikov photoaddition of methanol to 1,1-diphenylpropene sensitized by modified beta-cyclodextrin. *Chem. Commun.* **2006**, 1712-4. DOI PubMed
50. Fukuhara, G.; Mori, T.; Inoue, Y. Competitive enantiodifferentiating anti-Markovnikov photoaddition of water and methanol to 1,1-diphenylpropene using a sensitizing cyclodextrin host. *J. Org. Chem.* **2009**, *74*, 6714-27. DOI PubMed
51. Dong, J.; Liu, Y.; Cui, Y. Supramolecular chirality in metal-organic complexes. *Acc. Chem. Res.* **2021**, *54*, 194-206. DOI PubMed
52. Jin, Y.; Zhang, Q.; Zhang, Y.; Duan, C. Electron transfer in the confined environments of metal-organic coordination supramolecular systems. *Chem. Soc. Rev.* **2020**, *49*, 5561-600. DOI PubMed
53. Pan, M.; Wu, K.; Zhang, J.; Su, C. Chiral metal-organic cages/containers (MOCs): from structural and stereochemical design to applications. *Coord. Chem. Rev.* **2019**, *378*, 333-49. DOI
54. Li, K.; Zhang, L. Y.; Yan, C.; et al. Stepwise assembly of $\text{Pd}_6(\text{RuL}_3)_8$ nanoscale rhombododecahedral metal-organic cages via metalloligand strategy for guest trapping and protection. *J. Am. Chem. Soc.* **2014**, *136*, 4456-9. DOI PubMed
55. Wu, K.; Li, K.; Hou, Y. J.; et al. Homochiral D_4 -symmetric metal-organic cages from stereogenic Ru(II) metalloligands for effective enantioseparation of atropisomeric molecules. *Nat. Commun.* **2016**, *7*, 10487. DOI PubMed PMC
56. Guo, J.; Xu, Y. W.; Li, K.; et al. Regio- and enantioselective photodimerization within the confined space of a homochiral ruthenium/palladium heterometallic coordination cage. *Angew. Chem. Int. Ed. Engl.* **2017**, *56*, 3852-6. DOI PubMed
57. Guo, J.; Fan, Y. Z.; Lu, Y. L.; Zheng, S. P.; Su, C. Y. Visible-light photocatalysis of asymmetric [2+2] cycloaddition in cage-confined nanospace merging chirality with triplet-state photosensitization. *Angew. Chem. Int. Ed. Engl.* **2020**, *59*, 8661-9. DOI PubMed
58. Yoshizawa, M.; Tamura, M.; Fujita, M. Diels-alder in aqueous molecular hosts: unusual regioselectivity and efficient catalysis. *Science* **2006**, *312*, 251-4. DOI PubMed
59. Nishioka, Y.; Yamaguchi, T.; Kawano, M.; Fujita, M. Asymmetric [2 + 2] olefin cross photoaddition in a self-assembled host with remote chiral auxiliaries. *J. Am. Chem. Soc.* **2008**, *130*, 8160-1. DOI PubMed
60. Chen, J.; Wu, X.; Huang, S.; et al. Catalytic enantioselective cycloaddition transformation of tricyclic arenes enabled by a dual-role

- chiral cage-reactor. *ACS. Catal.* **2024**, *14*, 3733-41. DOI
61. Ruan, J.; Li, Z.; Yin, C.; et al. Enantioselective [2+2] cross-photocycloaddition enabled by a chiral cage reactor via multilevel-selectivity control. *ACS. Catal.* **2024**, *14*, 7321-31. DOI
62. Xiao, J. D.; Jiang, H. L. Metal-organic frameworks for photocatalysis and photothermal catalysis. *Acc. Chem. Res.* **2019**, *52*, 356-66. DOI PubMed
63. Wang, J.; Wang, C.; Lin, W. Metal-organic frameworks for light harvesting and photocatalysis. *ACS. Catal.* **2012**, *2*, 2630-40. DOI
64. Qiu, X.; Zhang, Y.; Zhu, Y.; et al. Applications of nanomaterials in asymmetric photocatalysis: recent progress, challenges, and opportunities. *Adv. Mater.* **2021**, *33*, e2001731. DOI PubMed
65. Chen, X. Y.; Chen, H.; Đorđević, L.; et al. Selective photodimerization in a cyclodextrin metal-organic framework. *J. Am. Chem. Soc.* **2021**, *143*, 9129-39. DOI PubMed
66. Wu, P.; He, C.; Wang, J.; et al. Photoactive chiral metal-organic frameworks for light-driven asymmetric α -alkylation of aldehydes. *J. Am. Chem. Soc.* **2012**, *134*, 14991-9. DOI PubMed
67. Xia, Z.; He, C.; Wang, X.; Duan, C. Modifying electron transfer between photoredox and organocatalytic units via framework interpenetration for β -carbonyl functionalization. *Nat. Commun.* **2017**, *8*, 361. DOI PubMed PMC
68. Zhang, Y.; Guo, J.; Shi, L.; et al. Tunable chiral metal organic frameworks toward visible light-driven asymmetric catalysis. *Sci. Adv.* **2017**, *3*, e1701162. DOI PubMed PMC
69. Hu, Y. H.; Liu, C. X.; Wang, J. C.; Ren, X. H.; Kan, X.; Dong, Y. B. $\text{TiO}_2@\text{UiO-68-CIL}$: a metal-organic-framework-based bifunctional composite catalyst for a one-pot sequential asymmetric Morita-Baylis-Hillman reaction. *Inorg. Chem.* **2019**, *58*, 4722-30. DOI PubMed
70. Wang, S.; Liu, W.; Wang, J.; et al. Mechanochemical encapsulation of enzymes into MOFs for photoenzymatic enantioselective catalysis. *ACS. Mater. Lett.* **2024**, *6*, 2609-16. DOI
71. Liu, W.; Yang, Y.; Yang, X.; et al. Template-directed fabrication of highly efficient metal-organic framework photocatalysts. *ACS. Appl. Mater. Interfaces.* **2021**, *13*, 58619-29. DOI PubMed
72. Kushnarenko, A.; Zabelina, A.; Guselnikova, O.; et al. Merging gold plasmonic nanoparticles and L-proline inside a MOF for plasmon-induced visible light chiral organocatalysis at low temperature. *Nanoscale* **2024**, *16*, 5313-22. DOI PubMed
73. Lee, J. M.; Cooper, A. I. Advances in conjugated microporous polymers. *Chem. Rev.* **2020**, *120*, 2171-214. DOI PubMed PMC
74. Yang, L.; Wang, J.; Zhao, K.; et al. Photoactive covalent organic frameworks for catalyzing organic reactions. *Chempluschem* **2022**, *87*, e202200281. DOI PubMed
75. Feng, X.; Ding, X.; Jiang, D. Covalent organic frameworks. *Chem. Soc. Rev.* **2012**, *41*, 6010-22. DOI PubMed
76. Ding, S. Y.; Wang, W. Covalent organic frameworks (COFs): from design to applications. *Chem. Soc. Rev.* **2013**, *42*, 548-68. DOI PubMed
77. He, T.; Zhao, Y. Covalent organic frameworks for energy conversion in photocatalysis. *Angew. Chem. Int. Ed. Engl.* **2023**, *62*, e202303086. DOI PubMed
78. Kang, X.; Stephens, E. R.; Spector-Watts, B. M.; et al. Challenges and opportunities for chiral covalent organic frameworks. *Chem. Sci.* **2022**, *13*, 9811-32. DOI PubMed PMC
79. Kang, X.; Wu, X.; Han, X.; Yuan, C.; Liu, Y.; Cui, Y. Rational synthesis of interpenetrated 3D covalent organic frameworks for asymmetric photocatalysis. *Chem. Sci.* **2019**, *11*, 1494-502. DOI PubMed PMC
80. Li, C.; Ma, Y.; Liu, H.; et al. Asymmetric photocatalysis over robust covalent organic frameworks with tetrahydroquinoline linkage. *Chinese. J. Catal.* **2020**, *41*, 1288-97. DOI
81. Zhou, Z.; Li, L.; Dai, L.; Liu, H.; Li, Y.; Li, P. The synthesis of highly crystalline covalent organic frameworks via the monomer crystal induction for the photocatalytic asymmetric α -alkylation of aldehydes. *J. Polym. Sci.* **2024**, *62*, 1621-8. DOI
82. Ma, H. C.; Sun, Y. N.; Chen, G. J.; Dong, Y. B. A BINOL-phosphoric acid and metalloporphyrin derived chiral covalent organic framework for enantioselective α -benzylation of aldehydes. *Chem. Sci.* **2022**, *13*, 1906-11. DOI PubMed PMC
83. He, T.; Liu, R.; Wang, S.; et al. Bottom-up design of photoactive chiral covalent organic frameworks for visible-light-driven asymmetric catalysis. *J. Am. Chem. Soc.* **2023**, *145*, 18015-21. DOI PubMed
84. Kan, X.; Wang, J. C.; Chen, Z.; et al. Synthesis of metal-free chiral covalent organic framework for visible-light-mediated enantioselective photooxidation in water. *J. Am. Chem. Soc.* **2022**, *144*, 6681-6. DOI PubMed
85. Ma, H. C.; Zhao, C. C.; Chen, G. J.; Dong, Y. B. Photothermal conversion triggered thermal asymmetric catalysis within metal nanoparticles loaded homochiral covalent organic framework. *Nat. Commun.* **2019**, *10*, 3368. DOI PubMed PMC
86. Ma, H. C.; Chen, G. J.; Huang, F.; Dong, Y. B. Homochiral covalent organic framework for catalytic asymmetric synthesis of a drug intermediate. *J. Am. Chem. Soc.* **2020**, *142*, 12574-8. DOI PubMed
87. Jin, C.; Li, N.; Lin, E.; et al. Enzyme immobilization in porphyrinic covalent organic frameworks for photoenzymatic asymmetric catalysis. *ACS. Catal.* **2022**, *12*, 8259-68. DOI